BMC Genomics

RESEARCH

Open Access

Physiological and transcriptomic analyses revealed the alleviating effects of exogenous Ca^{2+} and NO compound treatment on high salt stress in *Reaumuria soongorica*

Zehua Liu[1], Hanghang Liu[1], Bingbing Tan[1], Xidui Wang[1] and Peifang Chong[1*]

Abstract

Background Soil salinization represents the most prevalent abiotic stress, severely impacting a severe impact on plant growth and crop yield. Consequently, delving into the mechanism through which exogenous substances enhance plant salt tolerance holds significant importance for the stabilization and augmentation of crop yield.

Result In this study, within the context of salt stress, the seedlings of *R. soongorica* were subjected to exogenous Ca^{2+} and NO treatments. The aim was to comprehensively explore the alleviation effects of exogenous Ca^{2+} and NO on the high salt stress endured by *R. soongorica* from the perspectives of physiology and transcriptomics. The experimental results demonstrated that the combined treatment of exogenous Ca^{2+} and NO increased the relative water content and free water content of *R. soongorica* seedlings during salt stress conditions. Simultaneously, it induced a reduction in the leaf sap concentration, leaf water potential, water saturation deficit, and the ratio of bound water to free water. These modifications effectively regulated water metabolism and mitigated physiological drought induced by salt stress. In addition, the concurrent treatment of exogenous Ca^{2+} and NO could diminish Na^{+} and Cl^{-} levels in *R. soongorica* seedlings under salt stress. At the same time, it was effective in elevating the contents of K^{+} and Ca^{2+}, thereby facilitating the adjustment of the ion equilibrium. As a result, this treatment served to relieve the ion toxicity precipitated by salt stress, which is crucial for maintaining the physiological homeostasis and viability of the seedlings. Transcriptional analysis revealed that 65 differentially expressed genes (DEGs) were observable at three distinct stress time points in the context of high salt stress. Additionally, 154 DEGs were detected at three stress time points during the combined treatment. KEGG enrichment analysis revealed that phenylpropanoids biosynthesis, plant hormone signal transduction, MAPK signalling pathway, brassinosteroid biosynthesis and zeatin biosynthesis were significantly enriched under high salt stress and exogenous Ca^{2+} and NO compound treatment. Furthermore, WGCNA uncovered that multiple genes, including ADK, SBT, F-box protein, MYB, ZIP, PAL, METTL, and LRR, were implicated in the adaptive and mitigating mechanisms associated with the combined treatment of exogenous Ca^{2+} and NO in modulating high salt stress within *R. soongorica* seedlings.

Conclusion The outcomes of this study are highly conducive to disclosing the mechanism through which the combined treatment of exogenous Ca^{2+} and NO ameliorates the salt tolerance of *R. soongorica* from both physiological and transcriptional aspects. It also paves a solid theoretical groundwork for the employment of biotechnology in the breeding of *R. soongorica*, thereby offering valuable insights and a scientific basis for further research

*Correspondence:
Peifang Chong
zhongpf@gsau.edu.cn

and practical applications in enhancing the plant's ability to withstand salt stress and for the development of more salt-tolerant varieties of *R. soongorica*.

Keywords *Reaumuria soongorica*, Calcium, Nitric oxide, Salt stress, Physiology, Transcriptomics

Introduction

Salt stress, which is an abiotic stressor, has a direct and significant impact on plant growth and development. As the salt concentration in the soil steadily and continuously rises, plants are consequently subjected to high levels of salt stress. Studies have demonstrated that high salt stress can induce a reduction in plant photosynthesis, the suppression of protein synthesis, and the generation of reactive oxygen species (ROS). These consequences subsequently give rise to oxidative stress, ion toxicity, and malnutrition, ultimately culminating in detrimental effects on plant growth [1]. In addition, the accumulation of salt results in a soil acid–base imbalance that reduces permeability reduces land production efficiency and destroys the soil's ecological balance [2]. At present, the issue of global land salinization is growing increasingly severe. It acts as a significant impediment to the growth and development of plants, thereby disrupting the stability of the ecosystem [3]. This result, in turn, triggers a cascade of ecological and environmental problems. These include the acceleration of land desertification, exacerbation of soil erosion, a steep decline in forest cover, and a problematic reduction in biodiversity [4]. Salinization increases the difficulty of effectively using land resources, leading to the degradation or loss of soil ecosystem functions, severely restricting the sustainable development of human agricultural production and the ecological environment [5]. Therefore, enhancing the salt tolerance of plants holds profound and far-reaching significance when it comes to the rational utilization of salinized land. A high-salt environment greatly harms plant growth [6]. Scholars have reported that the logic and sensible application of plant growth regulators are effective methods for improving the salt resistance of plants [7].

Calcium ions (Ca^{2+}) play an essential role as the second messenger in plant growth, development, and stress response. Under abiotic stress, exogenous Ca^{2+} can alleviate the stress environment's inhibitory influence on plant cell growth and development. It actively contributes to the integrity of the plant cell structure, thereby ensuring the cells' ability to carry out their normal functions [8]. When plants are under salt stress, Ca^{2+} channel proteins, important salt signal receptors, can rapidly sense and sharply increase the intracellular Ca^{2+} concentration [9]. When the Ca^{2+} concentration required by plants under normal conditions is applied to plants under salt stress, plants lack Ca^{2+}. Adding a high amount of exogenous Ca^{2+} can alleviate plant deficiency symptoms, thus maintaining the basic structure and function of the plasma membrane and ensuring the standard transmission of the Ca^{2+} signalling system under salt stress [10]. Ca^{2+} is also a necessary factor for photosynthetic oxygen release. Exogenous Ca^{2+} can significantly increase plants' chlorophyll content and net photosynthetic rate under salt stress [11]. Nitric oxide (NO), a crucial signalling molecule within the realm of plants, assumes a pivotal and critical role in the plant's response mechanisms to both biotic and abiotic stresses [12]. Many reports have investigated the fact that NO has been shown to alleviate seeds' germination rate and germination index under salt stress and promote the absorption of beneficial nutrients by plants [13, 14]. In addition, NO can reverse the effects of salt stress on plant photosynthesis [15] and reduce salt stress damage by increasing the contents of proline, betaine and soluble sugars in plants [16] and regulating antioxidant metabolic pathways [17, 18]. Relevant studies have documented that nitric oxide (NO) partakes in the positive modulation of abscisic acid (ABA) accumulation in rice (*Oryza sativa*) and maize (*Zea mays*) when subjected to salt stress [19]. NO can also regulate the adaptability of perennial ryegrass (*Festuca arundinacea*) to salt stress by reducing Na^{+} accumulation and improving growth and photochemical efficiency [20]. Ca^{2+} and NO have emerged as prevalent substances with the capacity to enhance plant salt tolerance. Intriguingly, prior investigations have indicated that the homeostasis of Ca^{2+} within plant cells is under the regulatory influence of NO. NO achieves this by stimulating intracellular Ca^{2+}-permeable channels as well as plasma membrane channels, thereby facilitating the generation of Ca^{2+} in plant cells [21]. Therefore, the combined treatment using Ca^{2+} and NO is likely to exhibit a more favorable effect in alleviating the abiotic stress endured by plants than the application of a single substance. Nevertheless, to date, there has been a lack of reported research focusing on enhancing the abiotic stress tolerance of plants through the specific combination of Ca^{2+} and NO.

Reaumuria soongarica is a highly xerophytic salt-secreting shrub of the genus *Reaumuria* in Tamaricaceae. It has strong drought resistance, sand fixation, and water and soil conservation capabilities, and it plays a significant role in ecological protection and construction in desert and grassland areas [22]. Moreover, the leaves of *R. soongorica* are rich in protein, fat, and trace elements, making

this species a good forage in desert areas, where it can be used to graze sheep and camels. Therefore, *R. soongorica* is the primary species used in constructing forage shrubs and cultivating degraded grasslands [23]. The results highlighted that *R. soongorica* exhibits a relatively broad niche width across diverse salinity gradients as a characteristic salt-secreting plant. It can mitigate the adverse impacts of salt damage through the mechanisms of leaf salt secretion and the modulation of reactive oxygen species. However, drought and saline-alkali land are the main factors affecting the distribution of the *R. soongorica* community [24]. Research has shown that exogenous regulatory substances, including hydrogen sulfide, can slow the damage caused by high salt stress in *R. soongorica* seedlings by regulating the metabolism of reactive oxygen species [25]. Our previous preliminary experimental results revealed that the alleviation effect of Ca^{2+} and NO compound treatment on high salt stress in *R. soongorica* was significantly more significant than that of a single treatment with either Ca^{2+} or NO [26].

Further in-depth research has demonstrated that the exogenous application of Ca^{2+} and NO effectively attenuates the inhibitory influence of high salt stress on the growth of *R. soongorica* seedlings [26]. This attenuation is achieved by modulating the intricate processes of reactive oxygen species metabolism, carbon, and nitrogen metabolism. Transcriptomics can detect the overall transcriptional activity of any species at the single nucleotide level, especially non-model species such as *R. soongorica*. This technology can analyze gene expression levels more accurately and identify new transcripts and specific genes. Ying et al. [27] used the transcriptome to identify transcription factors differentially expressed under salt stress in *Glycyrrhiza infata*, including MYB, bZIP and NAC family. In *Rhododendron simii*, it was found that *RsWRKY40* is referred to salt tolerance by transcriptome analysis [28]. Therefore, the Illumina NovaSeq 6000 platform was used in this study to sequence the transcriptomes of *R. soongorica* seedlings treated with exogenous Ca^{2+} and NO under high salt stress. When integrated with the variation characteristics of phenotypic parameters, water metabolism, and ion content, the results served as a valuable source of basic data. This data was essential for comprehensively elucidating the molecular mechanism underlying the synergistic regulation of exogenous Ca^{2+} and NO in *R. soongorica* seedlings to relieve high salt stress.

Results

Effects of exogenous Ca^{2+} and NO compound treatment on the growth parameters of *R. soongarica* seeds under high salt stress

The results presented in Fig. 1 have been published in our previous paper [26]. We will better explain the growth parameters here to reveal the relationship between gene expression and growth traits. As shown in Fig. 1A, the growth differences of *R. soongorica* under various stresses can be observed. Beginning on the 9th day, compared with the control, high salt stress significantly reduced the plant height of *R. soongorica* seedlings ($P<0.05$), exogenous Ca^{2+} and NO alleviated salt stress, and the plant height was significantly higher in the high salt treatment than in the control (Fig. 1B). Moreover, it was observed that root length exhibited a higher degree of sensitivity to salt stress. In comparison with the control group (CK), salt stress notably diminished the root length of *R. soongorica* seedlings. This reduction became particularly conspicuous on the third day of treatment, registering a decrease of 3.88%. However, the exogenous application of Ca^{2+} and NO served to either decelerate or even reverse this inhibitory effect, thereby demonstrating these exogenous substances' potential to safeguard the seedlings' root growth and overall health under saline conditions (Fig. 1C). The changes in the stem diameter of *R. soongorica* seedlings with different stress times, high salt stress and exogenous Ca^{2+} and NO treatment were similar to those in plant height and root length (Fig. 1D). As the stress duration lengthened, the aboveground fresh weight of *R. soongorica* seedlings manifested a gradually increased. However, salt stress initiated adverse impacts on the ninth day of treatment. Notably, applying Ca^{2+} and NO led to a significant augmentation in the aboveground fresh weight under salt stress conditions, with an increase of 1.70% (Fig. 1E). High salt stress significantly reduced the aboveground dry weight of *R. soongorica* seedlings. Moreover, beginning on the 9th day of treatment, applying Ca^{2+} and NO highly increased the aboveground dry weight under salt stress. Still, both were lower than the control at the same time (Fig. 1F). On the 3rd day of stress, the fresh weight of the underground part of *R. soongorica* seedlings under high salt stress was not different from that of the control ($P>0.05$). On the 9th day of stress, the fresh weight of the underground part of *R. soongorica* seedlings under high salt stress was significantly lower than that of the control. Similarly, beginning on the 9th day of treatment, the application of Ca^{2+} and NO significantly increased the fresh weight of the underground part under salt stress (Fig. 1G). Beginning from the 9th day of treatment, it was evident that salt stress exerted a significant negative impact, leading to a notable reduction in the dry weight of the underground parts of *R. soongorica* seedlings. After the treatment with exogenous Ca^{2+} and NO, a significant augmentation was observed in the dry weight of the underground part of the plants when subjected to salt stress. Nevertheless,

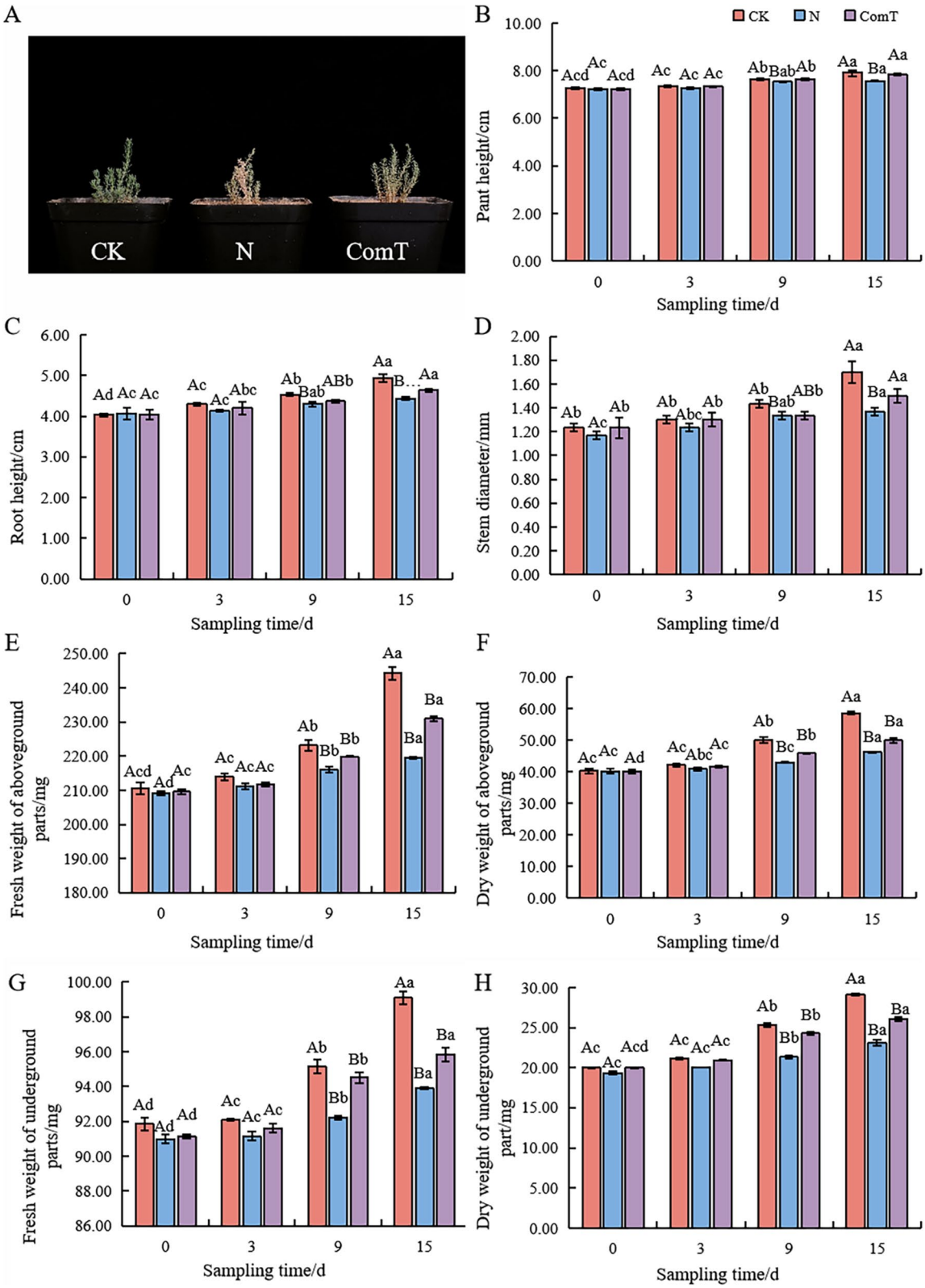

Fig. 1 Effect of exogenous Ca^{2+} and NO compound treatment on growth parameters of *Reaumuria soongarica* seedlings under high salt stress. Different capital letters indicate that the difference between various treatments at the same sampling time is significant, and different lowercase letters indicate that the difference between different times at the same treatment is substantial. The same is below

it is essential to note that both values remained lower than those of the control group during the identical period (Fig. 1H).

Effects of exogenous Ca^{2+} and NO compound treatment on the water metabolism of *R. soongarica* seeds under high salt stress

Figure 2 presents a vivid illustration of the alterations in the water metabolism of *R. soongorica* seedlings in response to diverse treatment regimens. Compared with the control, high salt stress significantly reduced the relative water content of *R. soongorica* seedlings ($P<0.05$). Compared with salt stress, the external application of Ca^{2+} and NO significantly increased the relative water content under salt stress. Still, both were lower than those in the control during the same period (Fig. 2A). In comparison with the condition under the control treatment, it was found that the water saturation deficit under high salt stress exhibited a significant elevation.

Conversely, when exogenous Ca^{2+} and NO treatment were applied, the water saturation deficit under salt stress was significantly reduced. However, it should be emphasized that the water saturation deficit under high salt stress remained notably more prominent than that under the control treatment during the same time frame, as depicted in Fig. 2B. The change in the bound water content was related to the stress period. At the 3-day mark, the content of bound water under high salt stress was marginally higher than that under the control treatment (CK). Additionally, the content of bound water under exogenous treatment was slightly more significant than that observed under salt stress. However, at fifteen days, a considerable divergence was noted. The content of bound water under high salt stress was substantially lower than that under CK.

In contrast, the content of bound water under the combined treatment with Ca^{2+} and NO was remarkably more significant than both that under high salt stress and the control, as clearly illustrated in Fig. 2C. Compared with the control, the free water content under high salt stress was significantly lower; however, after the combined treatment with Ca^{2+} and NO, the free water content of *R. soongorica* seedlings was markedly greater than that under high salt stress. Still, both were lower than the controls at the same time (Fig. 2D). Compared with the control group, high salt stress led to a strikingly significant increase in the bound water/free water ratio of *R. soongorica* seedlings.

In addition, at 0 and 3 days, the bound water/free water ratio in the combined treatment with exogenous Ca^{2+} and NO was significantly greater under salt stress (Fig. 2E). High salt stress significantly increased the leaf water potential of *R. soongorica*. In contrast, the leaf water potential of *R. soongorica* significantly decreased after the combined treatment with exogenous Ca^{2+} and NO. Still, both were considerably greater than the control at the same stress time (Fig. 2F). The variation tendency of the leaf sap concentration was in harmony with that of the leaf water potential. High salt stress brought about a notably significant elevation in the leaf sap concentration of *R. soongorica*. Specifically, it attained a peak of 13.89% at the 9-day mark. In contrast, compared with high salt stress, the leaf sap concentration of *R. soongorica* exhibited a significant decline following the combined treatment with exogenous Ca^{2+} and NO, as vividly depicted in Fig. 2G.

Effects of exogenous Ca^{2+} and NO compound treatment on the ion content of *R. soongarica* seedlings under high salt stress

The change in the ion content of *R. soongorica* seedlings was related to stress duration (Fig. 3). Compared with that in control, the content of Na^+ in the high-salt stress treatment significantly increased ($P<0.05$) and reached a maximum value of 1.04 $mmol \cdot g^{-1}$ at 9 days. Compared to the content of Na^+ in the high-salt stress treatment, a significant reduction was observed in the content of Na^+ in the mixed treatment involving exogenous Ca^{2+} and NO. However, it is essential to note that both values were greater than those in the control during the same period, as shown in Fig. 3A. The content of Cl^- under high salt stress was significantly greater than that under the control. The Cl^- content under the combination of exogenous Ca^{2+} and NO was considerably lower than that under the control treatment at the same time under salt stress (Fig. 3B). The content of K^+ under high salt stress was markedly lower than that in the control group. In contrast, the content of K^+ in the mixture of exogenous Ca^{2+} and NO was more excellent and significantly more remarkable than that under salt stress. Still, both were considerably lower than the controls at the same stress time (Fig. 3C).

Moreover, compared to the content of Ca^{2+} under the control treatment (CK), the content of Ca^{2+} under high salt stress was conspicuously lower. Additionally, the content of Na^+ under the combined treatment of exogenous Ca^{2+} and NO was remarkably more excellent than that under high salt stress and the control treatment during the same period (Fig. 3D). Compared with that under CK, the ratio of K^+/Na^+ under high salt stress significantly decreased, and the ratio of K^+/Na^+ under high salt stress increased dramatically under the combination treatment of exogenous Ca^{2+} and NO. Still, both were simultaneously lower than those under CK (Fig. 3E). Compared to the control, the ratio of $Ca^{2+}/Na+$ under high salt stress

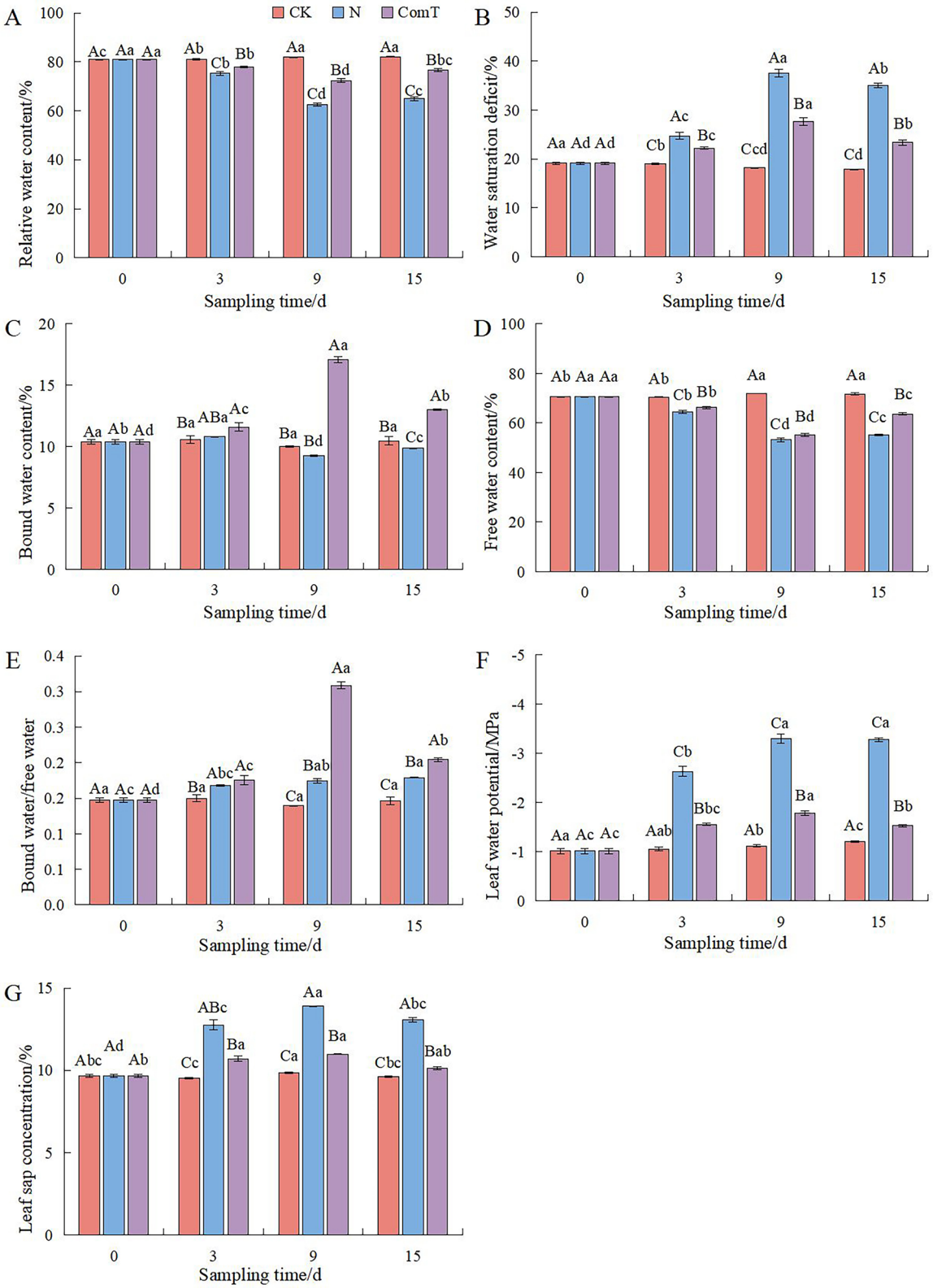

Fig. 2 Effect of exogenous Ca^{2+} and NO compound treatment on water metabolism of *R. soongarica* seedlings under high salt stress

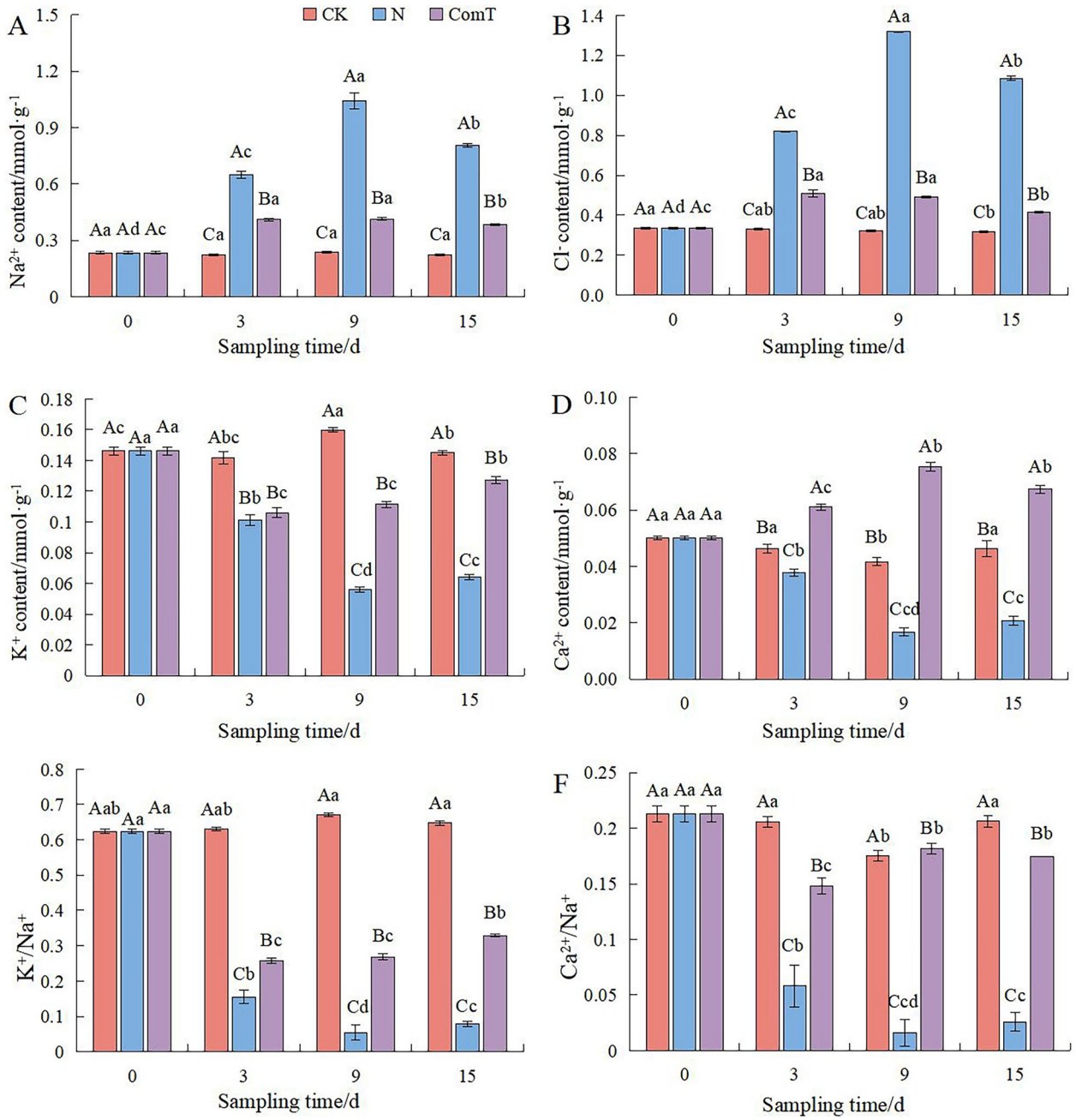

Fig. 3 Effect of exogenous Ca^{2+} and NO compound treatment on ion content of *R. soongarica* seedlings under high salt stress

was substantially lower. Notably, the ratio of K^+/Na^+ under high salt stress was significantly greater under the combined treatment with exogenous Ca^{2+} and NO. Except for the treatment with exogenous Ca^{2+} and NO for 9 days, the ratios at the other time points were lower than those in the control during the same period, as illustrated in Fig. 3F.

RNA quality inspection and sequencing results

The outcomes of the RNA quality inspection for the samples demonstrated that the total RNA of each of the 27 samples exhibited a high level of purity and integrity. The transcriptome sequencing results revealed that the number of clean bases in each sample was more significant than 6.14 GB, with an error rate of 0.0245% ~ 0.0284%, a

range that falls below 0.03%; the percentages of Q20 and q30 bases were 96.81% and 91.12%, respectively; and the percentage range of the GC content was 44.16% ~ 45.02% (Table 1). Further comparison of the clean reads revealed that the percentage of total mapped reads among the total reads of all the samples was more incredible than 68.71% (Table S1), indicating that the data quality of this study was high and could be used for subsequent analyses.

Transcriptome assembly and transcriptional functional annotation

The transcriptome assembly results revealed that the number of unigenes was 109,434, the number of transcripts was 202,755, and the average length of N50 was 1732 bp. Further analysis showed that 64.8% of the total BUSCO sequences were unigene sequences with the expected size, and 87.3% of the total BUSCO sequences were script sequences with the expected length, indicating that the unigene and script obtained in this study had high assembly integrity (Table S2). Statistical results revealed that unigene and transcript sequences with a 200–500 bp sequence length accounted for 40% and 34% of the total, respectively. The number of unigene and transcript sequences with a more than 4500 bp sequence length was the lowest, accounting for only 2.00% of the total (Fig. 4A and B). The BLAST search results revealed that the number of genes annotated to the NR database was the greatest, at 41,824, followed by those annotated to the GO database, at 3361 (Fig. 4C, Table S2). In addition, Venn diagram analysis revealed that 8362 genes, accounting for 19.56%, were annotated to the GO, KEGG, eggNOG, Pfam, NR, and Swiss-Prot databases. A total of 2285 genes were annotated only to the NR database, the highest number of individually annotated genes among all the databases (Fig. 4D).

Analysis and identification of DEGs

The number of DEGs in *R. soongorica* seedlings under high salt stress for different durations and under combined treatment with exogenous Ca^{2+} and NO was significantly different. Compared with those at 3 d

Table 1 Summary of transcriptome sequencing data and assembly results

Sample	Raw reads	Clean reads	Clean bases	Error rate(%)	(%)	(%)	GC content(%)	Mapped ratio
CK_3d1	45,649,668	43,755,730	6,464,800,865	0.0246	98.16	94.63	44.24	77.67%
CK_3d2	54,100,314	52,425,812	7,524,715,100	0.0247	98.16	94.66	44.74	81.11%
CK_3d3	44,929,982	43,758,824	6,531,141,668	0.0247	98.13	94.44	44.62	74.47%
NaCl_3d1	63,029,446	61,306,382	9,074,215,069	0.0246	98.17	94.63	44.58	75.87%
NaCl_3d2	53,174,234	51,806,866	7,680,210,818	0.0245	98.2	94.68	44.56	76.83%
NaCl_3d3	42,568,254	41,431,022	6,170,216,953	0.0246	98.17	94.62	44.57	75.95%
NaCl_NO_Ca_3d1	45,706,120	43,898,408	6,491,092,812	0.0246	98.14	94.63	44.27	78.62%
NaCl_NO_Ca_3d2	42,707,004	41,413,062	6,143,443,528	0.0245	98.21	94.75	44.42	77.77%
NaCl_NO_Ca_3d3	50,769,362	49,167,166	7,291,081,641	0.0246	98.17	94.66	44.38	78.60%
CK_9d1	45,429,250	44,423,352	6,478,856,652	0.0272	97.23	92.14	44.62	75.55%
CK_9d2	48,324,828	47,558,544	6,984,370,493	0.0275	97.13	91.84	44.69	74.57%
CK_9d3	52,921,884	51,877,042	7,609,771,601	0.0275	97.15	91.9	44.78	75.69%
NaCl_9d1	51,644,358	49,915,190	7,337,219,084	0.0281	96.87	91.4	44.54	76.35%
NaCl_9d2	49,783,208	47,890,586	7,049,235,868	0.0278	96.98	91.68	44.58	75.02%
NaCl_9d3	44,694,318	42,997,176	6,316,979,096	0.0281	96.86	91.37	44.6	77.37%
NaCl_NO_Ca_9d1	44,518,638	43,661,780	6,403,023,652	0.0281	96.91	91.35	44.76	74.85%
NaCl_NO_Ca_9d2	44,036,892	43,217,464	6,305,146,741	0.0277	97.06	91.66	44.74	76.61%
NaCl_NO_Ca_9d3	47,790,872	46,878,778	6,774,015,070	0.028	96.96	91.47	44.72	76.72%
CK_15d1	44,519,022	43,984,444	6,413,961,286	0.0269	97.36	92.37	44.73	77.61%
CK_15d2	45,347,670	44,534,818	6,526,020,373	0.0283	96.85	91.2	44.68	74.53%
CK_15d3	44,124,900	43,162,314	6,274,833,254	0.0276	97.11	91.83	44.65	75.54%
NaCl_15d1	69,446,722	67,406,450	9,818,215,434	0.0278	97.01	91.68	44.76	76.56%
NaCl_15d2	48,369,396	47,459,988	6,891,385,695	0.0284	96.81	91.12	44.84	76.13%
NaCl_15d3	43,292,360	42,572,696	6,219,598,480	0.0275	97.11	91.84	44.91	76.60%
NaCl_NO_Ca_15d1	51,183,178	50,405,450	7,374,251,215	0.0279	97	91.49	44.86	75.63%
NaCl_NO_Ca_15d2	50,812,204	50,073,672	7,339,278,207	0.0276	97.1	91.75	44.8	77.07%
NaCl_NO_Ca_15d3	56,511,812	55,553,608	8,147,523,329	0.0276	97.1	91.75	44.74	74.87%

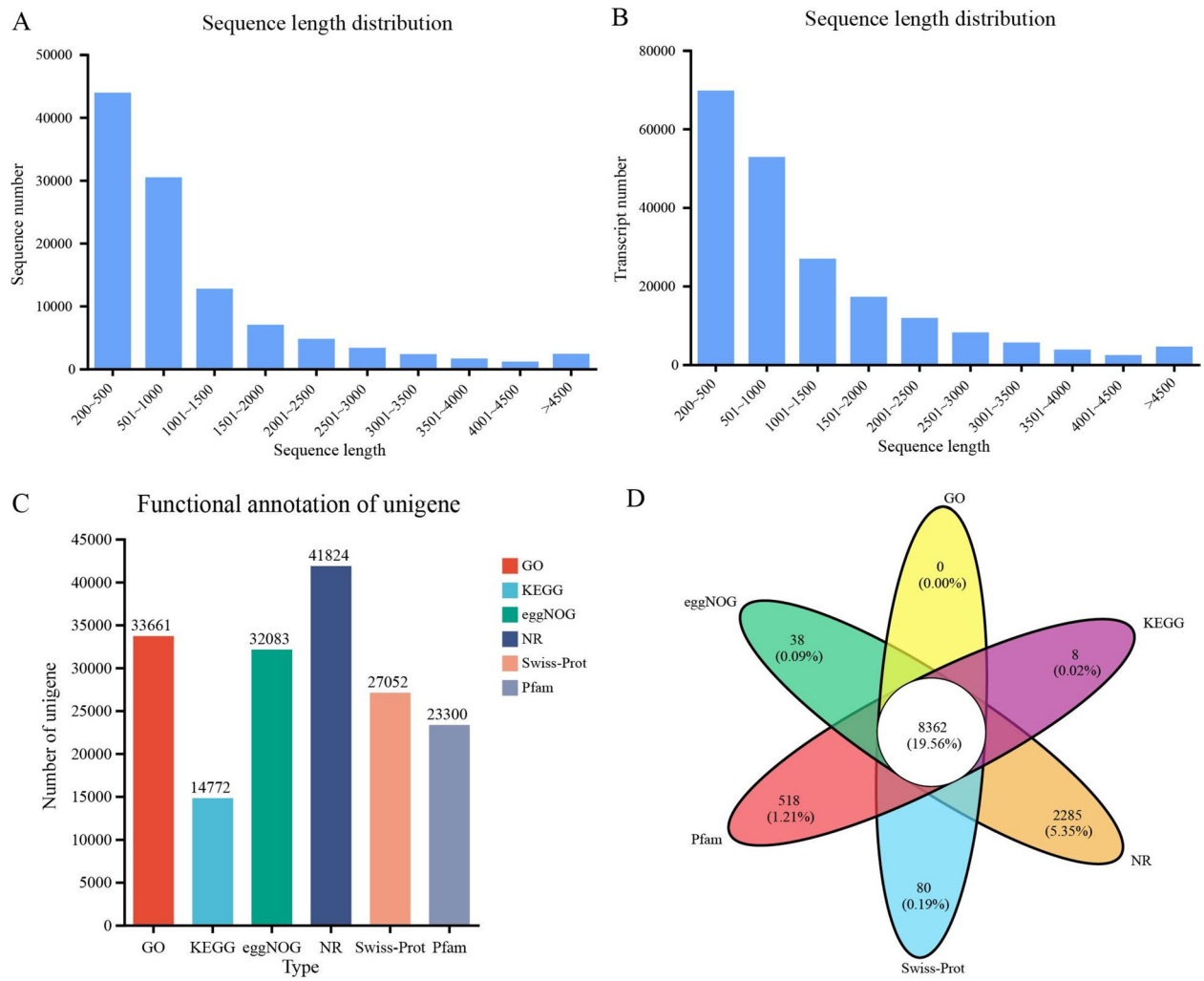

Fig. 4 Unigene and transcript assembly and database annotation. **A**: The length and quantity distribution of unigene; **B**: The length and quantity distribution of transcripts; **C**: Statistics of annotation results of 6 primary database functions; **D**: Venn diagram analysis of 6 database annotation results

and 15 d under salt stress, the number of upregulated DEGs identified at 9 d was the lowest, at only 72. Similarly, after exogenous Ca^{2+} and NO treatment under salt stress, the number of upregulated DEGs identified on the 9th day was still the lowest, with 183 genes. In addition, compared with those under high salt stress, the number of up-and downregulated genes decreased slightly after exogenous Ca^{2+} and NO compound treatment for 15 d, but the number of up-and downregulated genes increased significantly on Days 3 and 9; for example, the number of upregulated genes increased threefold-fold on Day 3 (Fig. 5A, Table S3). In the analysis of the specific genes expressed at the three treatment time points and intuitively identify the common and unique DEGs between salt stress and exogenous Ca^{2+} and NO treatment under salt stress, Venn diagram analysis revealed that there were only 30 genes in the six comparison groups (Fig. 5B, Figure S1). In addition, the study of all DEGs under high salt stress revealed 65 DEGs at three different stress time points, and the number of unique genes was most significant at 15 d, accounting for 77.09% (Fig. 5C). Venn diagram analysis of the effects of exogenous Ca^{2+} and NO compound treatment revealed that there were 154 genes at the three stress time points. Among the unique genes, the number was most significant at 15 d and lowest at 3 d (Fig. 5D).

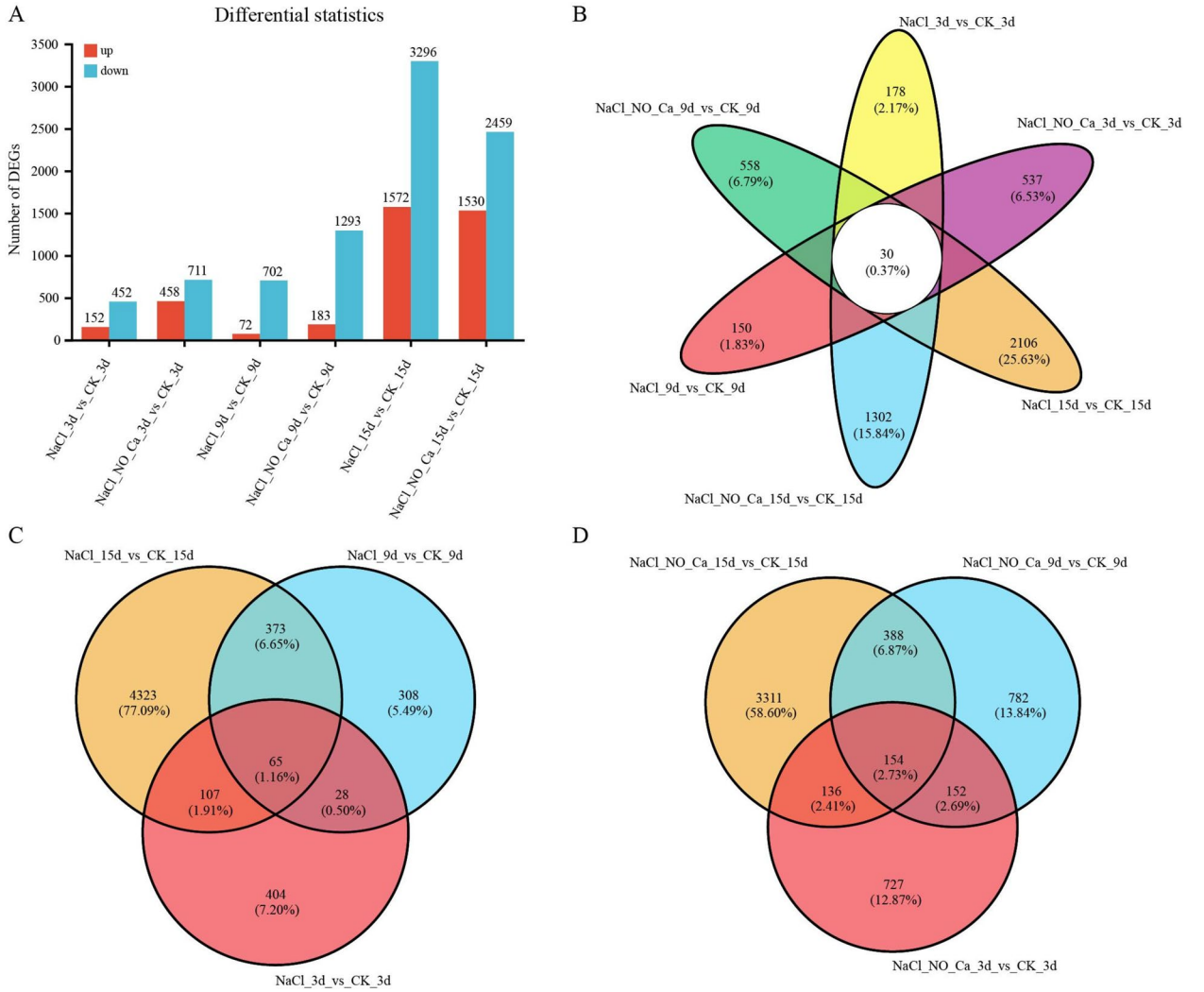

Fig. 5 Statistics of DEGs under different treatments and Venn plot analysis. **A** unigene quantity statistics under different treatments; **B**: Venn plot analysis of DEGs under different treatments; **C**: Venn plot analysis of DEGs under salt treatment; **D**: Venn plot analysis of DEGs under the combined treatment of exogenous Ca^{2+} and NO

DEG functional enrichment analysis GO enrichment analysis

The results revealed that, under high salt stress, the number of genes associated with metabolic processes and cellular processes was the greatest. The number of genes enriched with cell and membrane parts was the greatest among the cell components. Regarding biological processes, the number of genes associated with catalytic activities and binding was the most significant (Fig. 6A, C and E). When subjected to exogenous analysis, most GO terms were related to high salt stress (Fig. 6B, D and F). Still, the two groups differed in the number of enriched terms. At 3 and 9 d, the number of GO terms enriched with exogenous Ca^{2+} and NO was approximately twice that enriched with high-salt stress. However, the two groups had no significant difference in enriched terms at 15 d.

KEGG enrichment analysis

We performed the Kyoto Encyclopedia of Genes and Genomes (KEGG) enrichment analysis on the DEGs of different comparison groups. We selected the top 20 pathways with the lowest Q values for display (Fig. 7). Compared with the control, the enrichment pathways of *R. soongorica* under high salt stress were mainly flavonoid biosynthesis, glucosinolate biosynthesis, monoamide biosynthesis, tryptophan metabolism and so on. Under the combined treatment of exogenous Ca^{2+} and NO, the main enrichment pathways were anthocyanin biosynthesis; flavonoid biosynthesis; diphenyl-like, diarylheptane

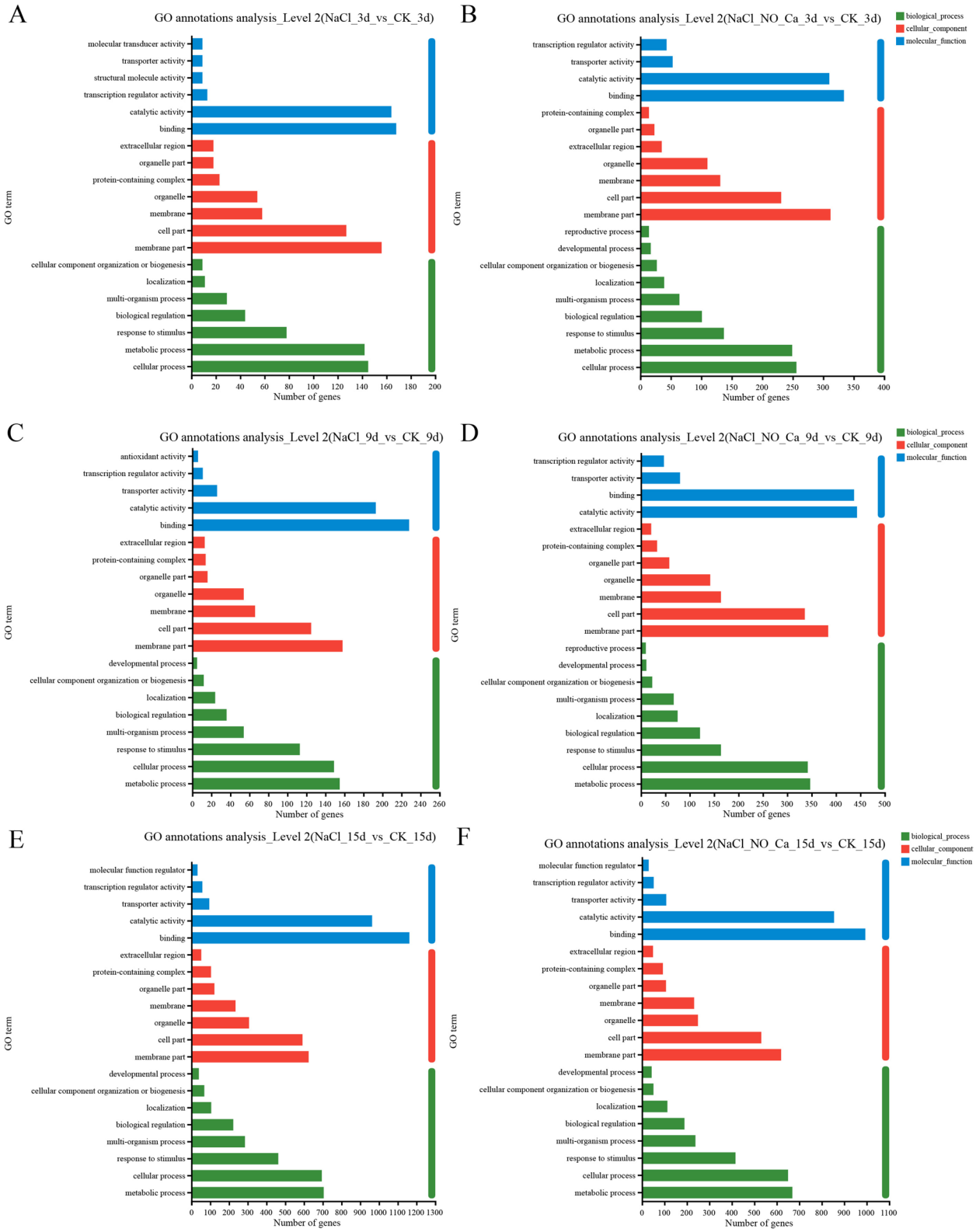

Fig. 6 GO enrichment analysis of DEGs under high salt stress and combined treatment for 3 d, 9 d and 15 d

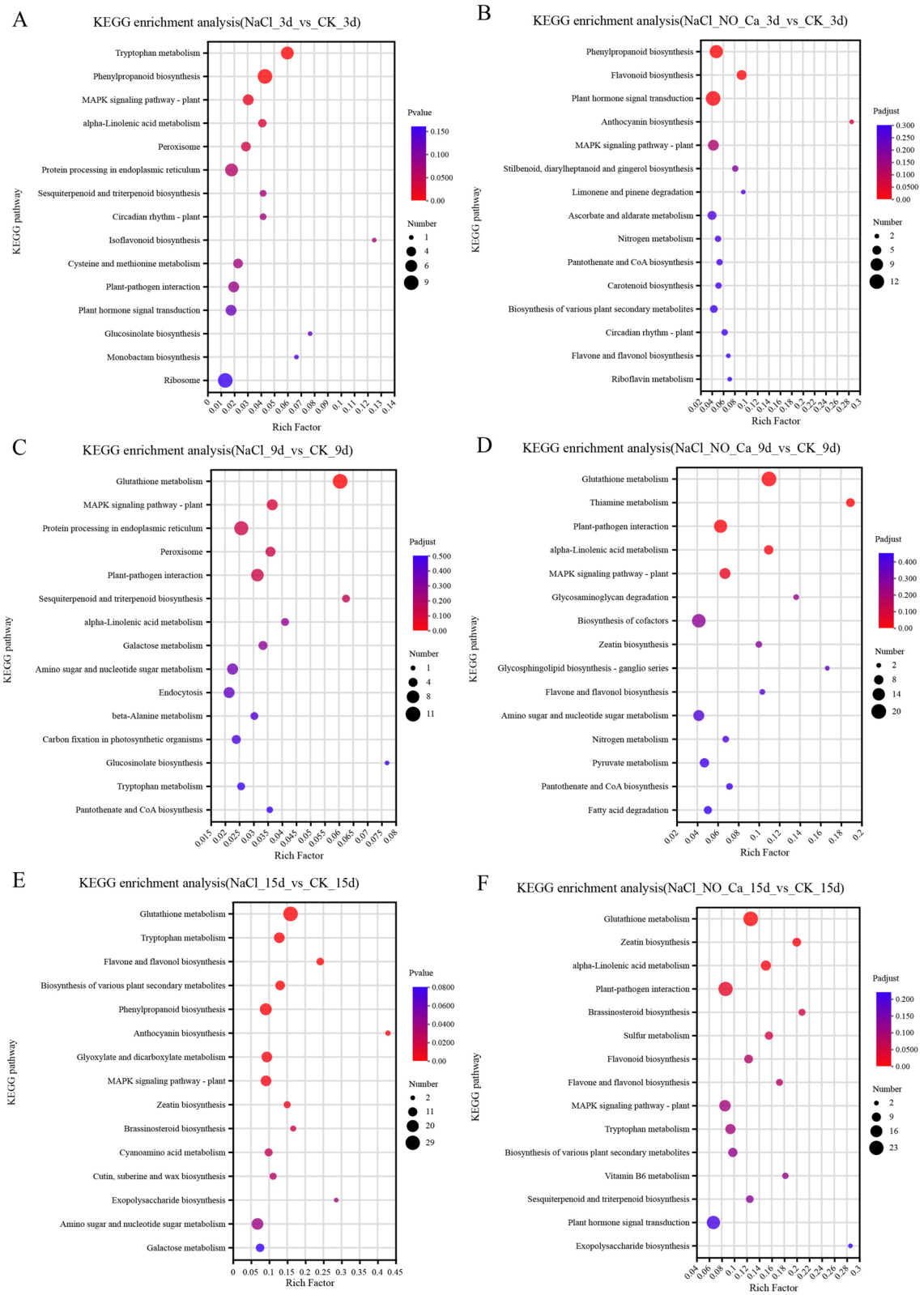

Fig. 7 KEGG enrichment analysis of DEGs on days 3, 9 and 15 under salt stress and combined treatment

and gingeroid biosynthesis; diarylheptanoid and gingerol biosynthesis; and limonene and pinene degradation (Fig. 7B). Among them, phenylpropanoid biosynthesis, plant hormone signal transduction and the MAPK signalling pathway were significantly enriched under high salt stress and exogenous Ca^{2+} and NO compound treatment. On the 9th day of treatment, the pathways associated with the accumulation of rhodopseudae under high salt stress were mainly glucosinolate biosynthesis, sesquiterpenoid and triterpenoid biosynthesis, glutathione metabolism and alpha-linolenic acid metabolism (Fig. 7C). Under the combined treatment with exogenous Ca^{2+} and NO, the main enriched pathways were thiamine metabolism, glycosphingolipid biosynthesis ganglion series, glycolytic glycan degradation and alpha-linolenic acid metabolism (Fig. 7D). The MAPK signalling pathway and plant and plant-pathogen interactions are shared among these pathways. At 15 d, the pathways enriched under high salt stress were anthocyanin biosynthesis, exopolysaccharide biosynthesis, flavonoid biosynthesis, brassinosteroid biosynthesis and so on. Under the combined treatment of exogenous Ca^{2+} and NO, the main enrichment pathways were exopolysaccharide biosynthesis, brassinosteroid biosynthesis, zeatin biosynthesis and vitamin B6 metabolism (Fig. 7F). Among them, the MAPK signalling pathway, plant pathway, zeatin biosynthesis pathway and brassinosteroid biosynthesis pathway are common.

Coexpression network analysis of high salt stress combined with exogenous Ca^{2+} and NO to alleviate high salt stress

Construction of the gene coexpression module

WGCNA represents a widely utilized approach for constructing a gene coexpression network. In this study, WGCNA was carried out on 27 samples obtained at three distinct stress time points during the imposition of high salt stress and the combined treatment of exogenous Ca^{2+} and NO (Fig. 8). The results obtained from the analysis disclosed that the gene expression information of each one of the samples was partitioned into 25 distinct gene coexpression modules, as illustrated in Fig. 8A. The number of genes encompassed within each gene coexpression module exhibited a pronounced disparity. The turquoise, grey, blue, brown, and yellow modules harbored a relatively more significant number of genes. In contrast, the dark grey, turquoise, dark green, and light

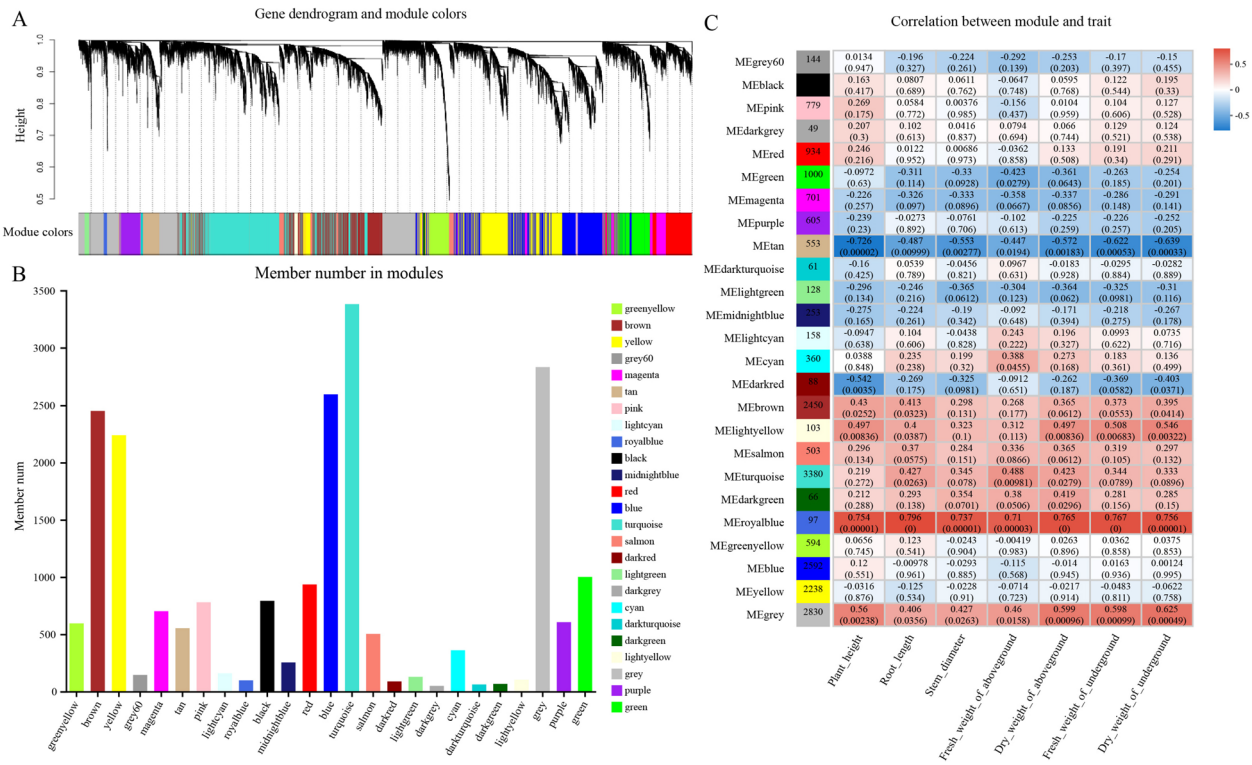

Fig. 8 WGCNA module division, gene number analysis, correlation analysis between modules, and phenotypic characteristics. **A** Hierarchical clustering analysis of coexpression genes; **B**: Analysis of the number of genes within the coexpression module; **C**: Heat map analysis of the correlation between coexpression modules and trait

yellow modules incorporated a comparatively smaller number of genes (Fig. 8B, Table S4).

Gene coexpression module construction and its association analysis with the phenotype

In the present study, 25 gene modules were employed to conduct an association analysis with the phenotypic traits that had been ascertained in the preceding phase, as depicted in Fig. 1. The outcomes of this analysis unveiled that seven phenotypic traits exhibited a significantly negative correlation with the tan module. The correlation coefficients in this regard ranged from −0.726 to −0.447. Moreover, it was observed that all of the phenotypic traits were notably and positively correlated with the royal blue module. This finding implies that the royal blue module was highly associated with the alterations in the phenotypic characteristics of *R. soongorica* under high salt stress conditions and the combined treatment of exogenous Ca^{2+} and NO. The genes encompassed within this module were principally engaged in the active promotion and positive modulation of the growth of *R. soongorica*. Analogously, the grey and light yellow modules also significantly and positively correlated with most phenotypic traits. The correlation coefficients within this range were between 0.312 and 0.599. The correlations between other modules and phenotypic characteristics were not high (Fig. 8C). Consequently, in the ensuing analysis, this research endeavoured to probe into the gene functions of these four modules. Specifically, it aimed to elucidate their responses to salt stress and the alleviating impact of the combined treatment of exogenous Ca^{2+} and NO.

Functional enrichment analysis of four related modules

The GO annotation analysis of the four gene modules significantly related to phenotype revealed that the molecular functions of the genes in the four gene modules were catalytic activity, transport activity, binding, transcriptional regulation activity, structural molecular activity, and molecular function regulation; cell components included cells, organelles, cell parts and membrane components; and biological processes included metabolic processes, multiple biological processes, cellular processes, responses to stimuli and biological regulation (Fig. 9).

KEGG annotation analysis revealed that the genes in the grey module were enriched mainly in phenylalanine metabolism and phenylpropane biosynthesis. The genes in the royal blue module were primarily annotated to be involved in thiamine metabolism, cysteine and methionine metabolism, ether lipid metabolism and biosynthesis in various plant secondary organisms. The genes in the light yellow module were annotated as being involved in oxidative phosphorylation and proteasome, starch and sucrose metabolism. The genes in the tan module were mainly annotated as being involved in tyrosine metabolism, sesquiterpene and triterpene biosynthesis, and amino sugar and nucleotide sugar metabolism (Fig. 10).

Visual analysis of the hub genes in the gene module

To mine hub genes related to phenotypic traits, this study performed gene network visualization and gene connectivity analysis on the top 30 genes according to the weights of the grey, blue, light yellow and yellow–brown modules (Fig. 11, Table 2). The hub gene of the grey module was TRINITY_DN4274_c0_g1 (phenylalanine ammonia-lyase 1). The core genes of the royal blue module included TRINITY_DN10257_c0_g1 (adenylate kinase 1, ADK), TRINITY_DN21718_c0_g1 (subtilisin-like protein, SBT), TRINITY_DN21963_c0_g1 (F-box protein), TRINITY_DN23412_c0_g1 (MYB family transcription factor) and four zinc transporter genes (ZIP, TRINITY_DN26057_c0_g1, TRINITY_DN28219_c0_g1, TRINITY_DN5840_c0_g3, TRINITY_DN5858_c0_g1). The hub gene of the light yellow module is TRINITY_DN15020_c0_g1 (NADH dehydrogenase subunit 1). The core genes of the tan module are TRINITY_DN4596_c0_g1 (wall-associated receptor kinase-like 2), TRINITY_DN46548_c0_g2 (glutathione S-transferase zeta class, GLU), TRINITY_dn4927_c0_g1 (RING-H2 finger protein), TRINITY_dn86020_c0_g1 (methyltransferase erase like protein, METTL), and several receptor kinases rich in leucine repeats (LRR, TRINITY_DN11359_c0_g1, TRINITY_DN13516_c0_g1, TRINITY_DN1680_c2_g1, TRINITY_DN17563_c0_g1, TRINITY_DN18427_c0_g1, TRINITY_DN23283_c0_g1, TRINITY_DN35211_c0_g1, TRINITY_DN4512_c1_g1, TRINITY_DN5554_c0_g1, TRINITY_DN62171_c0_g1, TRINITY_DN74.

qRT–PCR validation of the transcriptome analysis

To further verify the authenticity and reliability of the transcriptome data, based on the results of WGCNA, 12 DEGs were selected from four key modules (royal blue, grey, light yellow and tan) for qRT–PCR experiments (Table S5). The results revealed that the variation trend of the relative gene expression level calculated via qRT–PCR was consistent with that determined via RNA-seq, and the correlation coefficient was very high ($R^2 = 0.8994$), indicating that the transcriptome data were reliable (Fig. 12).

Discussion

Effects of exogenous Ca^{2+} and NO on the water metabolism of *R. soongorica* seedlings under high salt stress

Changes in plant water metabolism are a direct response to plant stress. Halophytes can usually maintain high

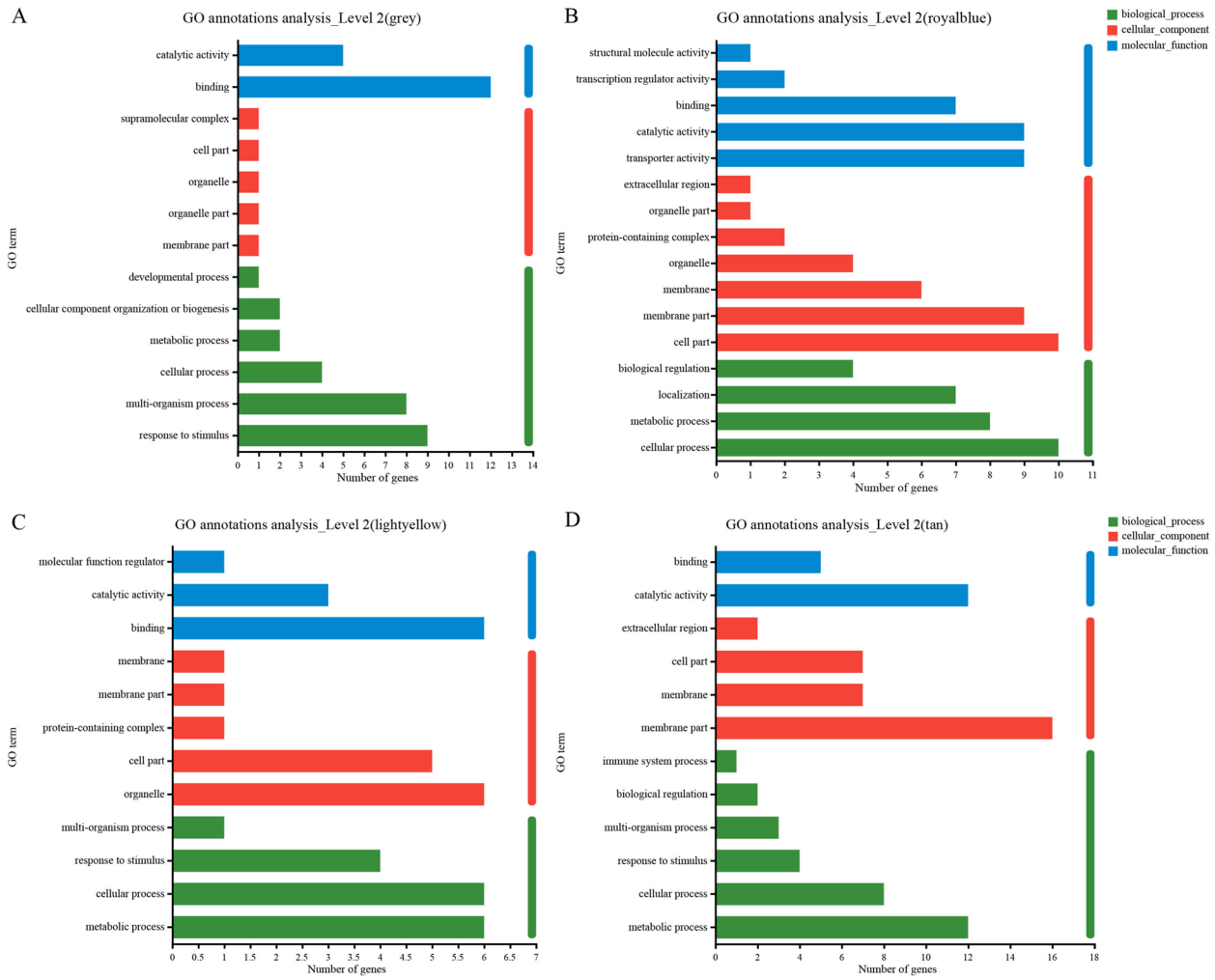

Fig. 9 GO enrichment analysis of significant correlation modules. **A** module grey; **B**: module royal blue; **C**: module light yellow; **D**: module tan. The same is below

water content under salt stress [29]. This study revealed that, compared with the control, high salt stress significantly reduced the relative water content of *R. soongorica* seedlings. In contrast, the external application of Ca^{2+} and NO significantly increased the water content under salt stress, similar to the findings in other plant species [30]. *R. soongorica* can also experience physiological drought under salt stress, and combined treatment with Ca^{2+} and NO can reduce the degree of cell water loss, but it cannot be eliminated. Arad and Richmond [31] reported that adding NaCl to the root medium of barley plants (*Hordeum vulgare* L.) markedly increased leaf RNase activity in parallel with an increase in leaf water saturation deficit. The results of this study are consistent with these findings. However, the exogenous Ca^{2+} and NO treatments significantly reduced the water saturation deficit. In addition, under salt stress, the free water content of *R. soongorica* decreased significantly, the bound water content did not change substantially, and the bound water/free water ratio increased significantly. After exogenous Ca^{2+} and NO combination treatment, the three parameters significantly increased, indicating that the ability of the combination of Ca^{2+} and NO to mitigate high salt stress in *R. soongorica* is very complex and that the changes only in free water and bound water contents cannot be fully explained. Relevant studies reported that the leaf water potential of tomato (*Solanum lycopersicum*) seedlings tended to decrease with increasing salt concentration [32]. In contrast, the changes in the SAP concentration and leaf water potential of *R. soongorica* were the same; they significantly increased under salt stress and decreased after exogenous Ca^{2+} and NO treatment, indicating that this may be a specific response of different species to salt stress. Comprehensive analysis revealed that salt stress reduced the relative water content, free water content, leaf juice concentration and

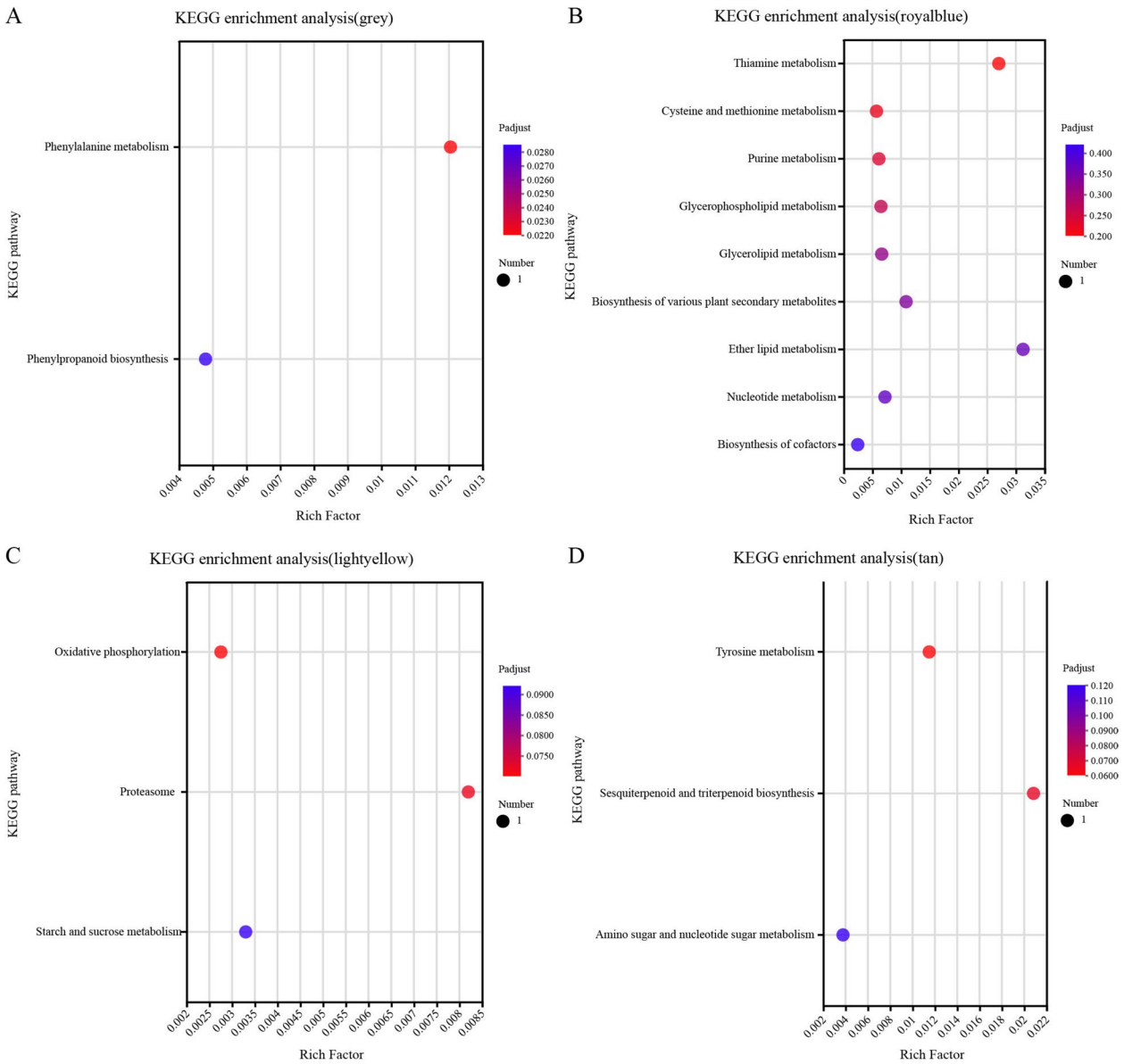

Fig. 10 KEGG enrichment analysis of significant correlation modules

water potential (both increased) and increased the water saturation deficit and bound water/free water ratio in *R. soongorica*. The combined treatment of Ca^{2+} and NO alleviated the salt stress of *R. soongorica* seedlings by regulating water-saving metabolism.

Effects of exogenous Ca^{2+} and NO compound treatment on the ion absorption of *R. soongorica* seedlings under high salt stress

Under salt stress, plants accumulate excessive Na^+ and Cl^-, resulting in osmotic ionic, and nutritional imbalances. Osmotic stress is caused by the rapid increase in salt concentration around roots in the early stage of salt stress, and the massive accumulation of Na^+ and Cl^- in the later stage leads to nutritional imbalance, which leads to ionic toxicity [33]. Plants are characterized by reducing water absorption by roots, metabolic dysfunction, inhibition of photosynthesis, and excessive accumulation of osmotic adjustment substances [34]. Na^+ has an ion hydration radius similar to that of K^+. Excessive Na^+ in plants affects the plants' absorption of K+. Under high salt concentrations, plants are subjected to the dual stresses of Na^+ toxicity and K^+ deficiency, thereby inhibiting enzymatic reactions [35, 36]. Under salt stress,

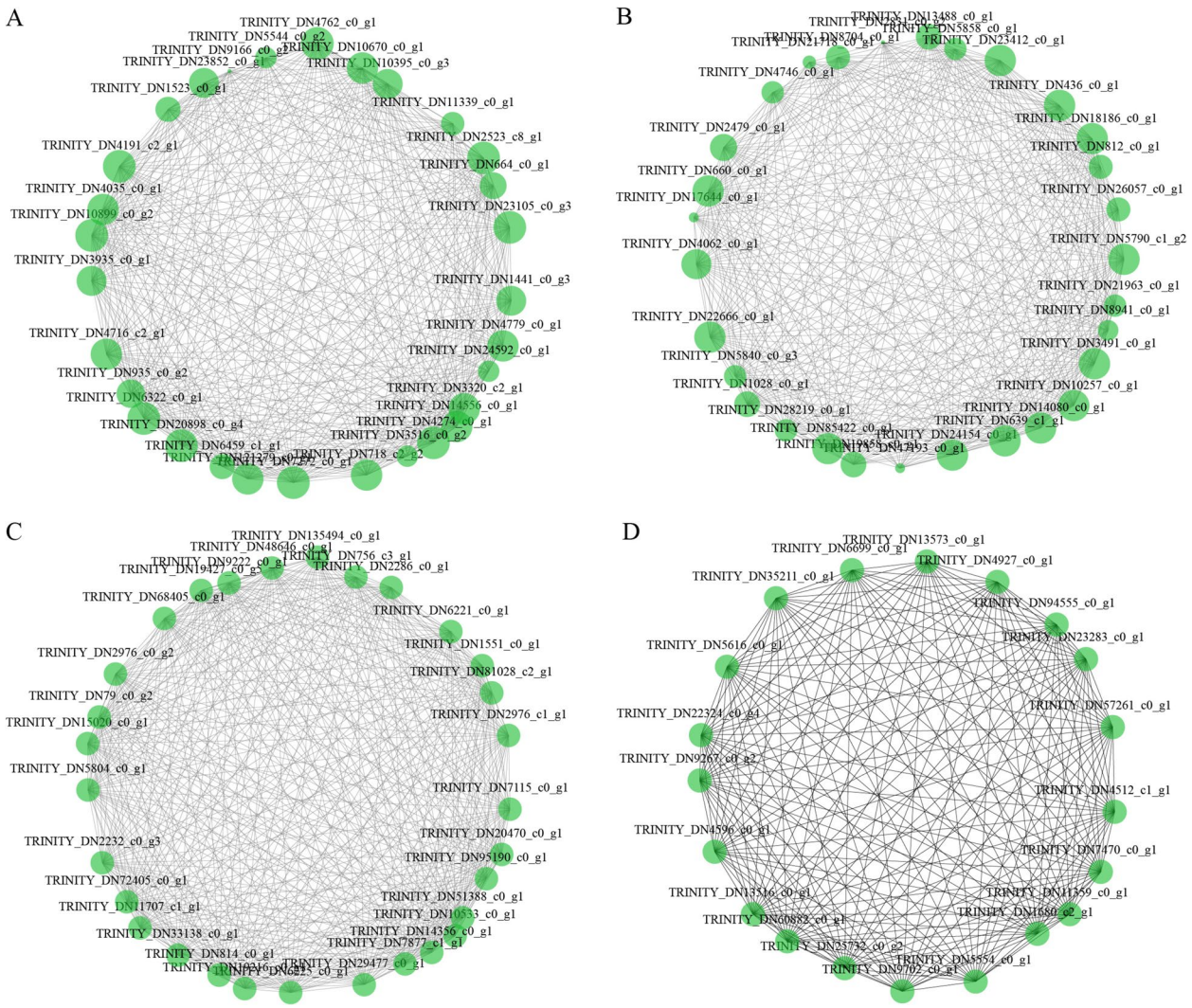

Fig. 11 Visual analysis of significant related modules. **A** module grey; **B**: module royal blue; **C**: module light yellow; **D**: module tan

the exogenous application of Ca^{2+} can improve the ion homeostasis and antioxidant defence of rice (*Oryza sativa*) seedlings and increase the tolerance of rice to salt stress [37]. The results revealed that the contents of Na^+ and Cl^- in *R. soongorica* seedlings significantly increased under salt stress and that the contents of Na^+ and Cl^- in *R. soongorica* seedlings significantly decreased after the combination treatment of exogenous Ca^{2+} and NO, indicating that the application of Ca^{2+} and NO can hinder the absorption of Na^+ and Cl^- by plants, thereby reducing the degree of salt stress damage. This study also revealed that the contents of K^+ and Ca^{2+} under high salt stress were significantly lower than those under the control conditions because *R. soongorica* absorbed too much Na^+ during salt treatment, which inhibited K^+ and Ca^{2+}. The contents of K^+ and Ca^{2+} increased significantly after the combination treatment with exogenous Ca^{2+} and NO, which was due to the exogenous supply of Ca^{2+}, and the increase in K^+ was due to the alleviation of ion toxicity caused by salt stress. In addition, the changes in the K^+/Na^+ and K^+/Na^+ ratios revealed that the ion balance destroyed by salt stress could be partially recovered after the combined treatment with Ca^{2+} and NO. The combined treatment of exogenous Ca^{2+} and NO effectively alleviated the ion toxicity caused by salt stress in *R. soongorica* and had a pronounced mitigating effect.

Differences in the number of DEGs under different durations of stress

At present, transcriptomics has been widely used in the study of plant salt resistance, which has revealed the functions of plant metabolic pathways and related genes,

Table 2 Candidate genes of mitigation of salt stress in *Reaumuria soongarica* by exogenous Ca^{2+} and NO Compound Treatment

Work Name	Gene Id	Description	15 d		9 d		3 d	
			NaCl_NO_Ca^{2+} vs CK	NaCl vs CK	NaCl_NO_Ca^{2+} vs CK	NaCl vs CK	NaCl_NO_Ca^{2+} vs CK	NaCl vs CK
ADK	TRINITY_DN10257_c0_g1	Adenylate kinase 1, chloroplastic-like	up	up	up	up	up	down
SBT	TRINITY_DN21718_c0_g1	Subtilisin-like protease SBT3.13	up	down	up	down	up	up
F-box gene	TRINITY_DN21963_c0_g1	F-box protein	up	up	up	down	up	up
MYB	TRINITY_DN23412_c0_g1	Myb family transcription factor EFM	up	down	up	up	up	up
ZIP	TRINITY_DN26057_c0_g1	Zinc transporter 1-like	up	down	up	down	up	down
ZIP	TRINITY_DN28219_c0_g1	Zinc transporter 4	up	down	up	down	up	down
ZIP	TRINITY_DN5840_c0_g3	Zinc transporter 1	up	down	up	down	up	down
ZIP	TRINITY_DN5858_c0_g1	Zinc transporter 1-like	up	down	up	down	up	down
PAL	TRINITY_DN4274_c0_g1	Phenylalanine ammonia-lyase 1	up	up	up	up	down	up
E3 ligase gene	TRINITY_dn4927_c0_g1	RING-H2 finger protein ATL29	down	down	down	down	down	down
METL protein	TRINITY_DN86020_c0_g1	Methyltransferase-like protein 7A	down	down	down	down	down	down
LRR-like proteins	TRINITY_DN11359_c0_g1	Receptor-like protein 6	down	down	down	down	down	down
LRR-like proteins	TRINITY_DN13516_c0_g1	Receptor-like protein 7	down	down	down	down	down	down
LRR-like proteins	TRINITY_DN1680_c2_g1	Receptor-like protein 33	down	down	down	down	down	down
LRR-like proteins	TRINITY_DN18427_c0_g1	Receptor-like protein 7	down	down	down	down	down	down
LRR-like proteins	TRINITY_DN23283_c0_g1	Receptor like protein 30-like	down	down	down	down	down	down
LRR-like proteins	TRINITY_DN4512_c1_g1	Receptor like protein 30-like	down	down	down	down	down	down
LRR-like proteins	TRINITY_DN62171_c0_g1	Receptor-like protein 12	down	down	down	down	down	down
LRR-like proteins	TRINITY_DN7470_c0_g1	Receptor like protein 30-like	down	down	down	down	down	down
LRR-like proteins	TRINITY_DN7504_c0_g2	Receptor like protein 30-like	down	down	down	down	down	down
LRR-like proteins	TRINITY_DN4596_c0_g1	Wall-associated receptor kinase-like 1	down	down	down	down	down	down

such as in wheat (*Triticum aestivum*) [38, 39], cotton (*Gossypium* spp.) [40], banana (*Musa paradisiaca*) [41] and tomato [42]. In addition, transcriptomics is widely used to study the mitigating effects of exogenous mitigators on plant salt stress, such as the increase in the salt resistance of *Nitraria tangutorum* seedlings caused by exogenous jasmonic acid [43] and the mitigating effect of exogenous calcium on millet (*Setaria italica*) salt stress [44]. In this study, *R. soongorica* seedlings subjected to different durations of stress were collected for high salt stress and exogenous Ca^{2+} and NO compound treatment to alleviate salt stress via transcriptome analysis. The results revealed that, compared with those under high salt stress, the number of up-and downregulated genes under Ca^{2+} and NO compound treatment at 3 and 9 d significantly increased, indicating that the stress duration was shorter and that the effects of Ca^{2+} and NO compound treatment may be alleviated by increasing gene expression. Compared with those under high salt stress, the number of up- and downregulated genes decreased

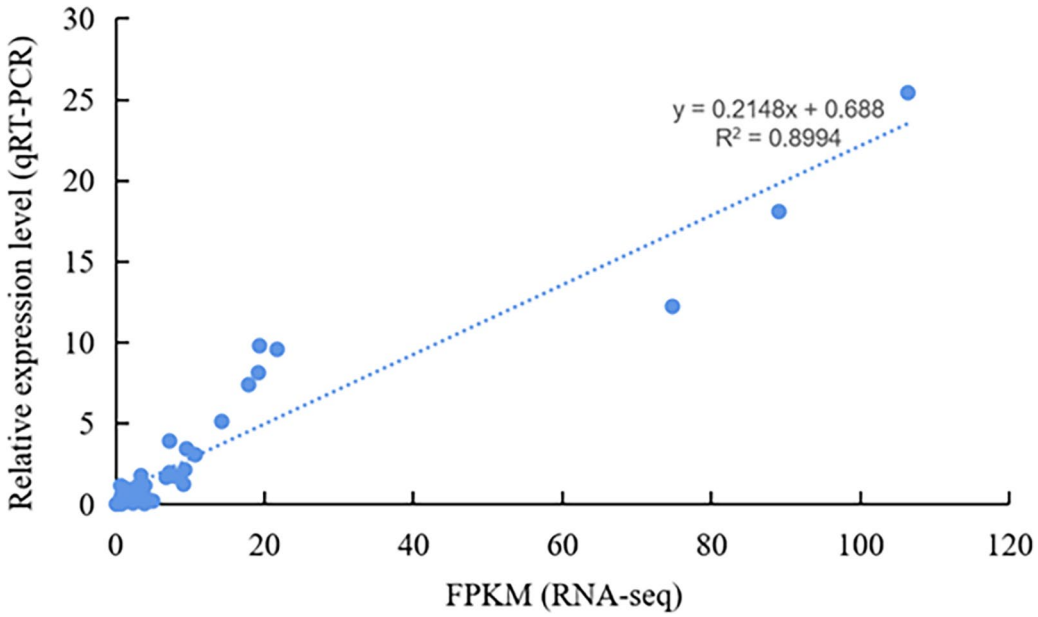

Fig. 12 Correlation analysis of RNA-seq. and qRT-PCR analysis results

slightly after treatment with exogenous Ca^{2+} and NO for 15 d, which showed that *R. soongorica* had been adapted to salt stress, so the number of genes mobilized by exogenous Ca^{2+} and NO was reduced. Therefore, the number of genes expressed under the combined treatment of exogenous Ca^{2+} and NO was not significantly different from that under high salt stress at 15 d.

Functional enrichment of DEGs

This study revealed that the GO terms and pathways for both classes of DEG (extraneous Ca^{2+} and NO compounds vs. Salt stress and Salt stress vs. CK) enrichment were essentially similar, which indicated that exogenous Ca^{2+} and NO did not affect the expression of many genes with new biological functions, mainly by altering the expression level of salt-tolerant genes or promoting the expression of related genes, to increase the salt tolerance of *R. soongorica* seedlings. The results of the GO analysis were rich and concentrated. The terms associated with significant enrichment after exogenous Ca^{2+} and NO combination treatment were the same as those related to high salt stress, including cell part, membrane part, metabolic process, cell process, catalytic activity and binding. The difference was that the number of DEGs associated with the same terms differed after treatment for 3 d and after treatment for 9 d. The number of DEGs associated with exogenous Ca^{2+} and NO combination treatment was approximately twice that related to high salt stress. These results were consistent with the number of DEGs identified, indicating that the combination of exogenous Ca^{2+} and NO alleviated the stress of *R. soongorica*, which was significantly correlated with the duration of stress.

The results of KEGG analysis were rich in anthocyanin biosynthesis; flavonoid biosynthesis; diphenyl-like, diarylheptane and gingeroid biosynthesis; diarylheptanoid and gingerol biosynthesis; limonene and pinene degradation; exopolysaccharide biosynthesis and other pathways, all of which were significantly enriched under the combined treatment of exogenous Ca^{2+} and NO. In addition, the pathways closely related to salt stress, such as phenylpropanoid biosynthesis, plant hormone signal transduction, the MAPK signalling pathway, brassinosteroid biosynthesis, zeatin biosynthesis and vitamin B6 metabolism, were significantly enriched under high salt stress and exogenous Ca^{2+} and NO compound treatment. The involvement of plant hormones in regulating plant salt tolerance has been widely reported [45]. For example, under salt stress, the content of cytokinin in cotton rapidly decreases [46]. The results of this study revealed the differential expression of genes in response to salt stress and the combination of exogenous Ca^{2+} and NO to alleviate multiple salt stress-induced hormone signalling pathways, including plant hormone signal transduction, brassinosteroid biosynthesis and zeatin biosynthesis, reflecting the complexity of the hormone signals involved in regulating the plant salt stress response. The MAPK signalling cascade pathway is essential in plant stress signal transduction. By predicting the interaction protein network of MAPK pathway genes that are differentially expressed in response to salt stress, multiple interactions,

such as between MAPK2 and MAPK4, which positively regulate the salt tolerance of *A. thaliana,* were identified [47]. In this study, the pathway with significant enrichment in KEGG was the MAPK signalling pathway, indicating that the combination of exogenous Ca^{2+} and NO alleviated the salt stress of *R. soongorica*, which was accompanied by the differential expression of genes related to the MAPK signalling pathway.

The molecular mechanism of treatment with exogenous Ca^{2+} and NO compounds on the salt stress of *R. soongorica* seedlings

The tolerance of plants to salt stress and the combined treatment of exogenous Ca^{2+} and NO to alleviate salt damage is achieved mainly by regulating the expression levels of related genes. Adenylate kinase (ADK) is a phosphotransferase that plays a vital role in maintaining the regular content of nucleotides in cells and energy metabolism activities and then regulates the corresponding stress of plants [48, 49]. Peterson et al. [50] treated the roots and stems of maize with two different ratios of Ca^{2+}/Na^{+} salt solutions. The results showed that ADK, which regulates adenylate metabolism, has an essential but complex relationship with plant salt stress. In this study, an adenosine monophosphate kinase gene (TRINITY_DN10257_c0_g1) was differentially expressed under different treatments, indicating that the combination of exogenous Ca^{2+} and NO could increase the tolerance of *R. soongorica* to salt stress by regulating the differential expression of ADK. In this study, the SBT gene (TRINITY_DN21718_c0_g1) was shown to regulate exogenous Ca^{2+} and NO compound treatment to alleviate the salt stress of *R. soongorica*. As the second most prominent member of the serine protease family, SBT has a wide variety and diverse functions. This protein is induced by plant salt stress [51, 52]. Most SBT genes can respond to plant salt stress [53]. F-box protein is widely involved in abiotic and abiotic stresses in plants and is regulated by a significant stress gene [52]. For example, Kumar and Kirti [54] reported that F-box protein is related to salt stress in peanuts (*Arachis hypogaea*). The interacting proteins of the salt-response factor *OsGRF7* include an F-BOX-containing protein (*OsFBO13*), which interacts to regulate salt stress in rice [55]. MYB transcription factors are involved in the *Arabidopsis* salt stress response and negatively regulate the response to salt stress by activating ABA signalling [56]. In the MYB family, *MYB3*, *MYB4*, *MYB13*, and *MYB59* were all involved in the wheat salt stress response, simultaneously acting on several downstream target genes associated with salt stress [57]. In this study, an F-box gene (TRINITY_DN21963_c0_g1) related to the phenotypic changes after salt stress and exogenous Ca^{2+} and NO combination treatment was obtained, indicating that the F-box gene may also play an active role in alleviating salt stress via Ca^{2+} and NO combination. MYB, as a large family, actively responds to plant abiotic stress. For example, the SlMYB102 gene is induced by salt stress and improves the salt tolerance of tomato salt tolerance by regulating ROS-scavenging enzyme accumulation [58]. In this study, a MYB gene (TRINITY_DN23412_c0_g1), which is involved in the process by which Ca^{2+} and NO compounds alleviate salt stress in *R. soongorica*, was also identified, and its specific regulatory mechanism needs to be further verified.

On the other hand, four ZIP genes (TRINITY_DN26057_c0_g1, TRINITY_DN28219_c0_g1, TRINITY_DN5840_c0_g3, TRINITY_DN5858_c0_g1) were identified via coexpression analysis. These results indicate that these genes combine exogenous Ca^{2+} and NO to alleviate the growth inhibition caused by salt stress and subsequently increase the salt tolerance of *R. soongorica*. Under high salt stress, *AtZTP29* may cause the UPR in cells by regulating the concentration of zinc in the endoplasmic reticulum, reducing the damage caused by unfolded proteins in the endoplasmic reticulum to cells, and improving the salt tolerance of plants [59]. AtHB23 is a HD-Zip class I transcription factor meditating *Arabidopsis* adaptation to salt stress by regulating primary and lateral root development [60]. After salt stress, the activity of the VcPAL enzyme in orchids is directly proportional to gene expression [61]. The expression of pal1 and PAL8 in *Nelumbo nucifera* was significantly upregulated under salt stress, which promoted the accumulation of flavonoids and other secondary metabolites [62]. Under salt stress, the PAL1 gene was overexpressed in pepper (Piper longum) roots, indicating that PAL1 responds positively to salt stress [63]. Wheat research has also achieved similar results [64]. The expression of the PAL gene and the change in PAL activity were closely related to salt stress. In this study, we identified a PAL gene (TRINITY_DN4274_c0_g1), which was differentially expressed when exogenous Ca^{2+} and NO compound treatment alleviated salt stress, indicating that the change in the PAL gene expression level is one of the mechanisms by which exogenous Ca^{2+} and NO compound treatment alleviates salt stress in *R. soongorica*. We should continue to determine PAL activity in subsequent studies to verify the role of PAL activity and its gene correlation in enhancing salt stress in *R. soongorica*.

Research has shown that ring-type ZIP plays an important role in the plant response to salt stress [65]. In addition, Guo et al. [66] and Stone and Callis [67] noted that E3 ligases containing rings are involved in the growth and development process and in the regulatory mechanism involved in the response to abiotic stress. In this study, we found that a ring containing the E3 ligase gene

(TRINITY_dn4927_c0_g1) plays a role in the exogenous Ca^{2+} and NO compound treatment process to alleviate the salt stress of *R. soongorica*. The biological process of this gene is ubiquitin-dependent protein catabolism, and its KEGG function is enriched in E3 ubiquitin ligases. Previous studies have shown that plants may respond to salt stress by regulating the level of DNA methylation and gene expression [68, 69]. In this study, we identified a METL protein (TRINITY_DN86020_c0_g1), which plays a role in alleviating the salt stress of *R. soongorica* under combined treatment with exogenous Ca^{2+} and NO, indicating that the change in the DNA methylation level may also be one of the reasons for the increased ability of *R. soongorica* to resist salt stress. Jung et al. [70] reported that *CaLRR1* was expressed rapidly not only after *Capsicum annuum* was infected with the anthrax pathogen but also under high salt stress, ABA treatment and other conditions to respond to stress. Lee et al. [71] noted that the *OsRLK1* gene in rice can be induced under low temperatures and under salt stress. In this study, 9 *LRR*-like proteins (TRINITY_DN11359_c0_g1, TRINITY_DN13516_c0_g1, TRINITY_DN1680_c2_g1, TRINITY_DN18427_c0_g1, TRINITY_DN23283_c0_g1, TRINITY_DN4512_c1_g1, TRINITY_DN62171_c0_g1, TRINITY_DN7470_c0_g1, TRINITY_DN7504_c0_g2), and a wall-associated receptor-like kinase (TRINITY_DN4596_c0_g1) were identified. These results indicate that these receptor-like kinases not only participate in the response of *R. soongorica* to salt stress but also alleviate the damage caused by salt stress by altering the expression levels of these genes under combined treatment with exogenous Ca^{2+} and NO. The above analysis revealed that at the transcriptional level, ADK, SBT, F-box protein, MYB, ZIP, PAL, METTL and other related genes are involved in the adaptation and mitigation mechanisms of exogenous Ca^{2+} and NO compound treatment in controlling high salt stress in *R. soongorica* seedlings.

Conclusion

This study comprehensively analyzed the physiological and transcriptome alterations in *R. soongorica* seedlings under high salt stress conditions and the combined treatment of exogenous Ca^{2+} and NO. High salt stress can induce physiological drought and ion toxicity in *R. soongorica*. The concurrent application of Ca^{2+} and NO can modulate water metabolism in several ways. It achieves this by diminishing the relative and free water content while augmenting the leaf sap concentration, potential saturation deficit, and bound water/free water ratio. Additionally, it reduces the Na^+ and Cl^- contents and elevates the K^+ and Ca^{2+} contents, thereby regulating the ion balance and ultimately adjusting the adaptability of *R. soongorica* seedlings to salt stress. Through the utilization of WGCNA, it was uncovered that genes such as ADK, SBT, F-box protein, MYB, ZIP, PAL, METTL, and LRR are implicated in the adaptive and mitigating mechanisms of the exogenous Ca^{2+} and NO combined treatment in the regulation of high salt stress within *R. soongorica* seedlings. These findings offer valuable insights into the molecular and physiological responses of *R. soongorica* to salt stress and the potential protective role of exogenous substances, which could pave the way for developing strategies to enhance the plant's salt tolerance and overall survival in saline environments.

Materials and methods

Experimental materials and salt treatments

In this study, a typical salt-secreting plant, *R. soongorica,* was selected as the test material, and the method in our previous analysis was adopted. In brief, *R. soongorica* seeds of uniform size were chosen, disinfected with 1% sodium hypochlorite, and then sown in a pot filled with sterilized quartz sand (10 cm × 10 cm × 8.5 cm), with five seeds in each pot. The plants were cultured in an artificial climate chamber at 25 °C/h for 14 h, 22 °C/h for 10 h, a light intensity of 600 μmol^{-1} m^{-2}, and a relative humidity of 60%. The seedlings were irrigated with Hoagland nutrient solution every 5 d. After 90 d of growth, the seedlings with good and consistent growth were selected for experimental treatment. The concentrations of NaCl (marked as N), exogenous NO and Ca^{2+} were 400 $mmol \cdot L^{-1}$, 0.25 $mmol \cdot L^{-1}$ and 20 $mmol \cdot L^{-1}$, respectively; the ratio of Ca^{2+} to NO was 1:3 (marked as ComT), and these concentrations and ratios were obtained through preliminary test screening. Moreover, an equal volume of deionized water was used as a control (CK), and each treatment was repeated three times.

Index determination

Determination of water metabolism

The relative water content was determined via the drying and weighing method. The specific steps were as follows: 0.5 g of *R. soongorica* seedling leaves were taken, the fresh weight (W0) was determined, the weighed leaves were placed in distilled water for 24 h, the surface water was dried, the weight (W1) was determined, the saturated leaves were placed in the oven at 105 °C for 30 min, and the dry matter weight (W2) was determined after drying at 65 °C to a constant weight. The water saturation deficit, bound water content and free water content were determined according to the methods of Fujino et al. [72]. The leaf water potential was measured with a dew point water potential meter (psypro, Dianjiang Technology Co., Ltd., Shanghai, China). The leaf water potential before dawn and afternoon was measured at 6:00 and 14:00, respectively. The change in leaf water potential

was measured every 2 h from 7:00 to 21:00. The concentration of leaf sap was measured with a hand-held sugar meter (SR-1, Yueda Electromechanical Equipment Co., Ltd., Shandong, and China). During the measurement, the seedlings were wiped clean and placed on the juicer to squeeze out the juice; a small amount of juice was taken from the dropper and dropped into the hand-held sugar meter for measurement.

Determination of the ion content

The *R. soongorica* seedlings were washed with distilled water, placed in an oven at 105 °C for 30 min, and dried at 65 °C to a constant weight. The dried samples were ground into powder by a pulverizer and sieved through 100 mesh for ion content determination. Na^+ and K^+ contents were determined via the flame photometer method. Ca^{2+} content was determined via atomic absorption spectrometry (AA-1800F, Meixie Instrument Co., Ltd., Shanghai, China). Cl^- content was determined via ion chromatography (pic-10, Puren Instrument, Qingdao, China).

Transcriptome analysis

RNA extraction

To eliminate the differences caused by different growth times, 27 samples of *R. soongorica* seedlings were collected on days 3rd, 9th and 15th of treatment, frozen in liquid nitrogen and stored at −80 °C for transcriptomic analysis. A total RNA extraction kit (Tiangen, Beijing, China) was used to extract RNA from the collected *R. soongorica* seedlings. The concentration and purity of the RNA were detected via a NanoDrop 2000, and the integrity of the RNA was detected via agarose gel electrophoresis. The RIN value of the RNA was determined via an Agilent 5300 (total RNA = 1 μg, concentration ≥ 30 ng·μL^{-1}, RIN > 6.5, OD260/280 between 1.8 and 2.2).

Database construction and sequencing

After the RNA quality test of the sample was performed, magnetic beads with oligo (DT) and Ploya were used for A-T base pairing, and the mRNA was isolated from the total RNA for the analysis of transcriptome information. The mRNA was randomly broken into small fragments of approximately 300 bp by adding a fragmentation buffer. A small fragment of mRNA was used as a template, random primers were used under reverse transcriptase, and the mRNA was inverted to synthesize single-strand cDNA. Then, the two strands were synthesized to form a stable double-strand structure. An end repair mixture was used to fill the sticky end of the double-stranded cDNA structure into the flat back, and a base at the 3' end was added to connect the Y-shaped connector. After connecting to the adapter, the product was purified and sorted, and the sorted product was amplified via PCR to obtain the final library. After the library passed quality inspection, Shanghai Meiji Biotechnology Co., Ltd. was subjected to sequencing on the Illumina NovaSeq 6000 platform.

Bioinformatics credits

Trinity software (https://github.com/trinityrnaseq/trinityrnaseq/wiki) was used for assembling the clean data in this study, and translate software (http://hibberdlab.com/transrate/) was used for filtering and optimizing the transcript sequences. Redundant sequences were removed via sequence alignment clustering. BUSCO software (http://busco.ezlab.org) was used to assess transcriptome integrity. The transcripts obtained were subsequently compared with six databases (NR, Swiss-Prot, Pfam, COG, GO and KEGG databases) via the Blastx algorithm to obtain the annotation information in each database, and the annotation situation of each database was statistically analysed.

RSEM software (http://deweylab.github.io/RSEM/) was used for quantitative analysis and FPKM conversion. After read counts were obtained, DESeq2 software (http://bioconductor.org/packages/stats/bioc/DESeq2/) was used for differentially expressed gene (DEG) analysis, and the screening criteria were FDR < 0.05 and |log2FC| ≥ 1. Goatools software (https://github.com/tanghaibao/GOatools) was subsequently used for GO enrichment analysis, and KOBAS (http://kobas.cbi.pku.edu.cn/home.do) was used for KEGG pathway enrichment analysis.

Weighted gene coexpression network analysis (WGCNA)

The Meiji bio-cloud platform (https://cloud.majorbio.com/) was used for the WGCNA of 27 samples at three stress time points under high salt stress and exogenous Ca^{2+} and NO compound treatment. The minimum number of genes in the module was set to 30, the merging threshold of similar modules was set to 0.25, and the modules with a similarity of 0.8 were merged. The other parameters were set to their defaults. After the coexpression network was generated, Cytoscape 3.9.1 and the Cytonca plug-in were used to draw the network diagram for the key nodes among the top 30 nodes regarding connectivity within the module.

qRT–PCR validation

Based on the results of WGCNA, 12 DEGs were selected from four key modules (royal blue, grey, light yellow and tan) for qRT–PCR further to verify the authenticity and reliability of the transcriptome data. Gene-specific primers were designed with Premier 5.0 software (Table S5). The real-time fluorescent quantitative PCR system was 20 μL in volume, amplified via a two-step method. The

samples were pre-denatured at 94 °C for 5 min, denatured at 95 °C for 15 s, and annealed at 60 °C for 30 s for 40 cycles. The relative expression of each gene was calculated via the $2^{-\Delta\Delta CT}$ method [73], and *Actin* was used as the internal reference gene.

Data analysis

SPSS 22.0 software was used for statistical analysis, single-factor ANOVA was used to analyse and process multiple groups of samples, Duncan's new multiple extreme difference method was used for significant analysis of variance, and Microsoft Excel 2007 was used for drawing and data processing.

Supplementary Information

The online version contains supplementary material available at https://doi.org/10.1186/s12864-025-11355-w.

Supplementary Material 1.
Supplementary Material 2.
Supplementary Material 3.
Supplementary Material 4.
Supplementary Material 5.
Supplementary Material 6.

Authors' contributions

ZHL and PFC conceived and designed the experiment. ZHL, HHL, BBT and XDW performed the experiments. ZHL and HHL analyzed all the data. ZHL wrote the manuscript. PFC revised the manuscript. All of the authors read and approved the final manuscript.

Funding

This study was funded by the Youth Doctoral Support Project for Universities in Gansu Province (2024QB-073).

Data availability

The original contributions presented in the study are publicly available. This data can be found here: National Center for Biotechnology Information (NCBI) BioProject database under accession number PRJNA1136819.

Declarations

Ethics approval and consent to participate

Experimental research and studies on plants in this study, including the collection of plant material, comply with the institutional, national, and international guidelines and legislation. Seeds of *R. soongarica* were collected in Laohukou, Wuwei, Gansu Province, China (102°58′ E, 38°44′ N; elevation 1315–1375 m), in late October 2019. This sampling area's average annual temperature, rainfall, and evaporation are 7.5 °C, 110 mm and 2, 646 mm, respectively. The seeds (voucher number: 063–2) were identified by Dr. X. Liu at the Institute of the Gansu Minqin National Studies Station for Desert Steppe Ecosystems (MSDSE). Seed samples were deposited at the Herbarium of the Scientific Research Experimental Station of the Longqu Seed Orchard, Gansu Province Academy of Qilian Water Resource Conservation Forests Research, in Zhangye. Plant materials were collected per the Technical Regulations for the Seed Collection of Rare and Endangered Wild Plants of the People's Republic of China (LYT2590-2016).

Consent for publication

Not applicable.

Competing interests

The authors declare no competing interests.

Author details

[1]College of Forestry, Gansu Agricultural University, Gansu Province, Yingmencun, Anning District, Lanzhou 730070, China.

Received: 9 October 2024 Accepted: 11 February 2025
Published online: 22 February 2025

References

1. Yadav S, Irfan M, Ahmad A, Hayat S. Causes of salinity and plant manifestations to salt stress: A review. Journal of environmental biology / Academy of Environmental Biology, India. 2011;32:667–85.
2. Barkla B, Castellanos T, Díaz De León Jl, Matros A, Mock H-P, Pérez-Alfocea F, et al. Elucidation of salt stress defense and tolerance mechanisms of crop plants using proteomics-Current achievements and perspectives. Proteomics. 2013;13:1885–900.
3. Zhu Y, Gong H. Beneficial effects of silicon on salt and drought tolerance in plants. Agron Sustain Dev. 2014;34(2):455–72.
4. Zhu YX, Gong HJ, Yin JL. Role of Silicon in Mediating Salt Tolerance in Plants: A Review. Plants (Basel, Switzerland). 2019;8(6):147.
5. Nishiuchi S, Fujihara K, Liu S, Takano T. Analysis of expressed sequence tags from a NaHCO3-treated alkali-tolerant plant, Chloris virgata. Plant physiology and biochemistry : PPB / Société française de physiologie végétale. 2010;48:247–55.
6. van Zelm E, Zhang Y, Testerink C. Salt Tolerance Mechanisms of Plants. Annu Rev Plant Biol. 2020;71:403–33.
7. Yang Y, Guo Y. Elucidating the molecular mechanisms mediating plant salt-stress responses. New Phytol. 2018;217(2):523–39.
8. Mockevičiūtė R, Jurkonienė S, Šveikauskas V, Zareyan M, Jankovska-Bortkevič E, Jankauskienė J, Kozeko L, Gavelienė V. Probiotics, Proline and Calcium Induced Protective Responses of Triticum aestivum under Drought Stress. Plants (Basel, Switzerland). 2023;12(6):1301.
9. Steinhorst L, He G, Moore LK, Schültke S, Schmitz-Thom I, Cao Y, Hashimoto K, Andrés Z, Piepenburg K, Ragel P, et al. A Ca(2+)-sensor switch for tolerance to elevated salt stress in Arabidopsis. Dev Cell. 2022;57(17):2081–2094.e2087.
10. Paunov M, Koleva L, Vassilev A, Vangronsveld J, Goltsev V. Effects of Different Metals on Photosynthesis: Cadmium and Zinc Affect Chlorophyll Fluorescence in Durum Wheat. International journal of molecular sciences. 2018;19(3):787.
11. Epstein E. How calcium enhances plant salt tolerance. Science (New York, NY). 1998;280(5371):1906–7.
12. Moreau M, Lee GI, Wang Y, Crane BR, Klessig DF. AtNOS/AtNOA1 is a functional Arabidopsis thaliana cGTPase and not a nitric-oxide synthase. J Biol Chem. 2008;283(47):32957–67.
13. Duan P, Ding F, Wang F, Wang BS: Priming of seeds with nitric oxide donor sodium nitroprusside (SNP) alleviates the inhibition on wheat seed germination by salt stress. Zhi wu sheng li yu fen zi sheng wu xue xue bao = Journal of plant physiology and molecular biology 2007, 33(3):244–250.
14. Huang J, Zhu C, Hussain S, Huang J, Liang Q, Zhu L, Cao X, Kong Y, Li Y, Wang L et al: Effects of nitric oxide on nitrogen metabolism and the salt resistance of rice (Oryza sativa L.) seedlings with different salt tolerances. Plant physiology and biochemistry : PPB 2020, 155:374–383.
15. Sami F, Siddiqui H, Alam P, Hayat S: Nitric Oxide Mitigates the Salt-Induced Oxidative Damage in Mustard by UpRegulating the Activity of Various Enzymes. J Plant Growth Regul. 2021;40:2409–32.
16. Ren Y, Wang W, He J, Zhang L, Wei Y, Yang M: Nitric oxide alleviates salt stress in seed germination and early seedling growth of pakchoi (Brassica chinensis L.) by enhancing physiological and biochemical parameters. Ecotoxicology and environmental safety 2020, 187:109785.
17. Ahmad P, Abdel Latef AA, Hashem A, Abd Allah EF, Gucel S, Tran LS. Nitric Oxide Mitigates Salt Stress by Regulating Levels of Osmolytes and Antioxidant Enzymes in Chickpea. Front Plant Sci. 2016;7:347.
18. Liu H, Li C, Yan M, Zhao Z, Huang P, Wei L, Wu X, Wang C, Liao W. Strigolactone is involved in nitric oxide-enhanced the salt resistance in tomato seedlings. J Plant Res. 2022;135(2):337–50.

19. Yi Y, Peng Y, Song T, Lu S, Teng Z, Zheng Q, Zhao F, Meng S, Liu B, Peng Y, et al. NLP2-NR Module Associated NO Is Involved in Regulating Seed Germination in Rice under Salt Stress. Plants (Basel, Switzerland). 2022;11(6):795.
20. Ji Z, Camberato J, Zhang C, Jiang Y. Effects of 6-Benzyladenine, γ-Aminobutyric Acid, and Nitric Oxide on Plant Growth, Photochemical Efficiency, and Ion Accumulation of Perennial Ryegrass Cultivars to Salinity Stress. HortScience. 2019;54:1418–22.
21. Lamotte O, Courtois C, Dobrowolska G, Besson-Bard A, Alain P, Wendehenne D. Mechanisms of nitric-oxide-induced increase of free cytosolic Ca2+ concentration in Nicotiana plumbaginifolia cells. Free Radical Biol Med. 2006;40:1369–76.
22. Yan S, Chong P, Zhao M, Liu H. Physiological response and proteomics analysis of Reaumuria soongorica under salt stress. Sci Rep. 2022;12(1):2539.
23. Zhang H, Liu X, Yang X, Wu H, Zhu J, Zhang H. miRNA-mRNA Integrated Analysis Reveals Roles for miRNAs in a Typical Halophyte, Reaumuria soongorica, during Seed Germination under Salt Stress. Plants (Basel, Switzerland). 2020;9(3):351.
24. Yan S, Chong P, Zhao M. Effect of salt stress on the photosynthetic characteristics and endogenous hormones, and: A comprehensive evaluation of salt tolerance in Reaumuria soongorica seedlings. Plant Signal Behav. 2022;17(1):2031782.
25. Liu H, Chong P, Liu Z, Bao X, Tan B. Exogenous hydrogen sulfide improves salt stress tolerance of Reaumuria soongorica seedlings by regulating active oxygen metabolism. PeerJ. 2023;11: e15881.
26. Liu Z, Liu H, Tan B, Wang X, Chong P. Mitigation of Salt Stress in Reaumuria soongarica Seedlings by Exogenous Ca2+ and NO Compound Treatment. Agronomy. 2023;13(8):2124.
27. Xu Y, Lu JH, Zhang JD, Liu DK, Wang Y, Niu QD, Huang DD. Transcriptome revealed the molecular mechanism of Glycyrrhiza inflata root to maintain growth and development, absorb and distribute ions under salt stress. BMC Plant Biol. 2021;21(1):599.
28. Guo LP, Mao X, Chen Y, Li L, Hu YR, Zhang HH, Zhang R, Wang YK: Transcriptome analysis reveals salt stress-related genes in Rhododendron simii and RsWRKY40 is referred to salt tolerance. Environ Exp Bot. 2024;220:105678.
29. Mann A, Lata C, Kumar N, Kumar A, Kumar A, Sheoran P. Halophytes as new model plant species for salt tolerance strategies. Front Plant Sci. 2023;14:1137211.
30. Zhu Y, Yin J, Liang Y, Liu J, Jia J, Huo H, Wu Z, Yang R, Gong H. Transcriptomic dynamics provide an insight into the mechanism for silicon-mediated alleviation of salt stress in cucumber plants. Ecotoxicol Environ Saf. 2019;174:245–54.
31. Arad SM, Richmond AE. Leaf cell water and enzyme activity. Plant Physiol. 1976;57(4):656–8.
32. Xue F, Liu W, Cao H, Song L, Ji S, Tong L, Ding R. Stomatal conductance of tomato leaves is regulated by both abscisic acid and leaf water potential under combined water and salt stress. Physiol Plant. 2021;172(4):2070–8.
33. Chen C, He G, Li J, Perez-Hormaeche J, Becker T, Luo M, Wallrad L, Gao J, Li J, Pardo JM, et al. A salt stress-activated GSO1-SOS2-SOS1 module protects the Arabidopsis root stem cell niche by enhancing sodium ion extrusion. EMBO J. 2023;42(13): e113004.
34. Tavakkoli E, Fatehi F, Coventry S, Rengasamy P, McDonald GK. Additive effects of Na+ and Cl- ions on barley growth under salinity stress. J Exp Bot. 2011;62(6):2189–203.
35. Shah FA, Ni J, Tang C, Chen X, Kan W, Wu L. Karrikinolide alleviates salt stress in wheat by regulating the redox and K(+)/Na(+) homeostasis. Plant physiology and biochemistry : PPB. 2021;167:921–33.
36. Rahman A, Nahar K, Hasanuzzaman M, Fujita M. Calcium Supplementation Improves Na(+)/K(+) Ratio, Antioxidant Defense and Glyoxalase Systems in Salt-Stressed Rice Seedlings. Front Plant Sci. 2016;7:609.
37. Rahnama A, James R, Poustini K, Munns R. Stomatal conductance as a screen for osmotic stress tolerance in durum wheat growing in saline soil. Funct Plant Biol. 2010;37:255–63.
38. Ma X, Gu P, Liang W, Zhang Y, Jin X, Wang S, Shen Y, Huang Z. Analysis on the transcriptome information of two different wheat mutants and identification of salt-induced differential genes. Biochem Biophys Res Commun. 2016;473(4):1197–204.
39. H E, My P, Okay S. Hexaploid wheat (Triticum aestivum L.) root miRNome analysis in response to salt stress. Ann Appl Biol. 2015;167(2):208–16.
40. Wei Y, Xu Y, Lu P, Wang X, Li Z, Cai X, Zhou Z, Wang Y, Zhang Z, Lin Z, et al. Salt stress responsiveness of a wild cotton species (Gossypium klotzschianum) based on transcriptomic analysis. PLoS ONE. 2017;12(5):e0178313.
41. Wei J, Liang J, Liu D, Liu Y, Liu G, Wei S. Melatonin-induced physiology and transcriptome changes in banana seedlings under salt stress conditions. Front Plant Sci. 2022;13: 938262.
42. Zhu X, Su M, Wang B, Wei X. Transcriptome analysis reveals the main metabolic pathway of c-GMP induced by salt stress in tomato (Solanum lycopersicum) seedlings. Functional plant biology : FPB. 2022;49(9):784–98.
43. Gao Z, Gao S, Li P, Zhang Y, Ma B, Wang Y. Exogenous methyl jasmonate promotes salt stress-induced growth inhibition and prioritizes defense response of Nitraria tangutorum Bobr. Physiol Plant. 2021;172(1):162–75.
44. Han F, Sun M, He W, Cui X, Pan H, Wang H, Song F, Lou Y, Zhuge Y. Ameliorating effects of exogenous Ca(2+) on foxtail millet seedlings under salt stress. Functional plant biology : FPB. 2019;46(5):407–16.
45. Ryu H, Cho Y-G. Plant hormones in salt stress tolerance. Journal of Plant Biology. 2015;58:147–55.
46. Yu Z, Duan X, Luo L, Dai S, Ding Z, Xia G. How Plant Hormones Mediate Salt Stress Responses. Trends Plant Sci. 2020;25(11):1117–30.
47. Teige M, Scheikl E, Eulgem T, Dóczi R, Ichimura K, Shinozaki K, Dangl JL, Hirt H. The MKK2 pathway mediates cold and salt stress signaling in Arabidopsis. Mol Cell. 2004;15(1):141–52.
48. Gong P, Zhang J, Li H, Yang C, Zhang C, Zhang X, Khurram Z, Zhang Y, Wang T, Fei Z, et al. Transcriptional profiles of drought-responsive genes in modulating transcription signal transduction, and biochemical pathways in tomato. J Exp Bot. 2010;61(13):3563–75.
49. Zhou S, Wei S, Boone B, Levy S. Microarray analysis of genes affected by salt stress in tomato. Afr J Environ Sci Technol. 2006;1(2):14–26.
50. Peterson TA, Nieman RH, Clark RA. Nucleotide Metabolism in Salt-Stressed Zea mays L. Root Tips: I. Adenine and Uridine Nucleotides. Plant physiology 1987;85(4):984–989.
51. Chichkova NV, Shaw J, Galiullina RA, Drury GE, Tuzhikov AI, Kim SH, Kalkum M, Hong TB, Gorshkova EN, Torrance L, et al. Phytaspase, a relocalisable cell death promoting plant protease with caspase specificity. EMBO J. 2010;29(6):1149–61.
52. Srivastava R, Liu JX, Howell SH. Proteolytic processing of a precursor protein for a growth-promoting peptide by a subtilisin serine protease in Arabidopsis. The Plant journal : for cell and molecular biology. 2008;56(2):219–27.
53. Hou QC, Wang LL, Qi YC, Yan TW, Zhang F, Zhao W, Wan XY. A systematic analysis of the subtilase gene family and expression and subcellular localization investigation of anther-specific members in maize. Plant Physiol Biochem. 2023;203:108041.
54. Kumar D, Kirti P. The genus Arachis: an excellent resource for studies on differential gene expression for stress tolerance. Front Plant Sci. 2023;14:1275854.
55. Chen YP, Dan ZW, Li SQ. GROWTH REGULATING FACTOR 7-mediated arbutin metabolism enhances rice salt tolerance. Plant Cell. 2024;36(8):2834–50.
56. Fang Q, Wang Q, Mao H, Xu J, Wang Y, Hu H, He S, Tu J, Cheng C, Tian G et al. AtDIV2, an R-R-type MYB transcription factor of Arabidopsis, negatively regulates salt stress by modulating ABA signaling. Plant Cell Rep. 2018;37:1499–511.
57. Sukumaran S, Lethin J, Liu X, Pelc J, Zeng P, Hassan S, Aronsson H. Genome-Wide Analysis of MYB Transcription Factors in the Wheat Genome and Their Roles in Salt Stress Response. Cells. 2023;12(10):1431.
58. Zhang X, Chen L, Shi Q, Ren Z. SlMYB102, an R2R3-type MYB gene, confers salt tolerance in transgenic tomato. Plant Sci. 2019;291:110356.
59. Wang M, Xu Q, Yu J, Yuan M. The putative Arabidopsis zinc transporter ZTP29 is involved in the response to salt stress. Plant Mol Biol. 2010;73(4–5):467–79.
60. Spies FP, Perotti MF, Cho YH, Jo CI, Hong JC, Chan RL. A complex tissue-specific interplay between the Arabidopsis transcription factors AtMYB68, AtHB23, and AtPHL1 modulates primary and lateral root development and adaptation to salinity. Plant J. 2023;115(4):952–66.
61. Xiang L, Moore BS. Characterization of benzoyl coenzyme A biosynthesis genes in the enterocin-producing bacterium "Streptomyces maritimus." J Bacteriol. 2003;185(2):399–404.
62. Chalabaev S, Turlin E, Bay S, Ganneau C, Brito-Fravallo E, Charles JF, Danchin A, Biville F. Cinnamic acid, an autoinducer of its own

biosynthesis, is processed via Hca enzymes in Photorhabdus luminescens. Appl Environ Microbiol. 2008;74(6):1717–25.
63. Shams M, Yuksel EA, Agar G, Ekinci M, Kul R, Turan M, Yildirim E. Biosynthesis of capsaicinoids in pungent peppers under salinity stress. Physiol Plan. 2023;175(2):e13889.
64. Moffitt MC, Louie GV, Bowman ME, Pence J, Noel JP, Moore BS. Discovery of two cyanobacterial phenylalanine ammonia lyases: kinetic and structural characterization. Biochemistry. 2007;46(4):1004–12.
65. Tian M, Lou L, Liu L, Yu F, Zhao Q, Zhang H, Wu Y, Tang S, Xia R, Zhu B, et al. The RING finger E3 ligase STRF1 is involved in membrane trafficking and modulates salt-stress response in Arabidopsis thaliana. The Plant journal : for cell and molecular biology. 2015;82(1):81–92.
66. Guo L, Nezames CD, Sheng L, Deng X, Wei N. Cullin-RING ubiquitin ligase family in plant abiotic stress pathways(F). J Integr Plant Biol. 2013;55(1):21–30.
67. Stone SL, Callis J. Ubiquitin ligases mediate growth and development by promoting protein death. Curr Opin Plant Biol. 2007;10(6):624–32.
68. Ferreira LJ, Azevedo V, Maroco J, Oliveira MM, Santos AP. Salt Tolerant and Sensitive Rice Varieties Display Differential Methylome Flexibility under Salt Stress. PLoS ONE. 2015;10(5): e0124060.
69. Wang M, Qin L, Xie C, Li W, Yuan J, Kong L, Yu W, Xia G, Liu S. Induced and constitutive DNA methylation in a salinity-tolerant wheat introgression line. Plant Cell Physiol. 2014;55(7):1354–65.
70. Jung EH, Jung HW, Lee SC, Han SW, Heu S, Hwang BK. Identification of a novel pathogen-induced gene encoding a leucine-rich repeat protein expressed in phloem cells of Capsicum annuum. Biochem Biophys Acta. 2004;1676(3):211–22.
71. Lee S-C, Kim J-Y, Kim SH, Kim S-J, Lee K, Han S-K, Choi H-S, Jeong D-H, An G, Kim S-R. Trapping and characterization of cold-responsive genes from T-DNA tagging lines in rice. Plant Sci. 2004;166:69–79.
72. Fujino M, Endo R, Omasa K. Nondestructive Instrumentation of Water-stressed Cucumber Leaves. Agricultural Information Research. 2002;11:161–70.
73. Livak KJ, Schmittgen TD. Analysis of relative gene expression data using real-time quantitative PCR and the 2-delta/delta (CT) method. Methods. 2001;25:402–8.

Publisher's Note